



Galaxy Clusters

(part II)

Elena Panko

I.I. Mechnikov Odessa National University
Odessa, Ukraine

Modern situation

Wild-field digitized surveys and Automatic Procedure:
objective search galaxy "overdense" regions

Pencil-beam observations (deep fields)

Red shift surveys

X-ray surveys

Numerical simulations!

Mock catalogues

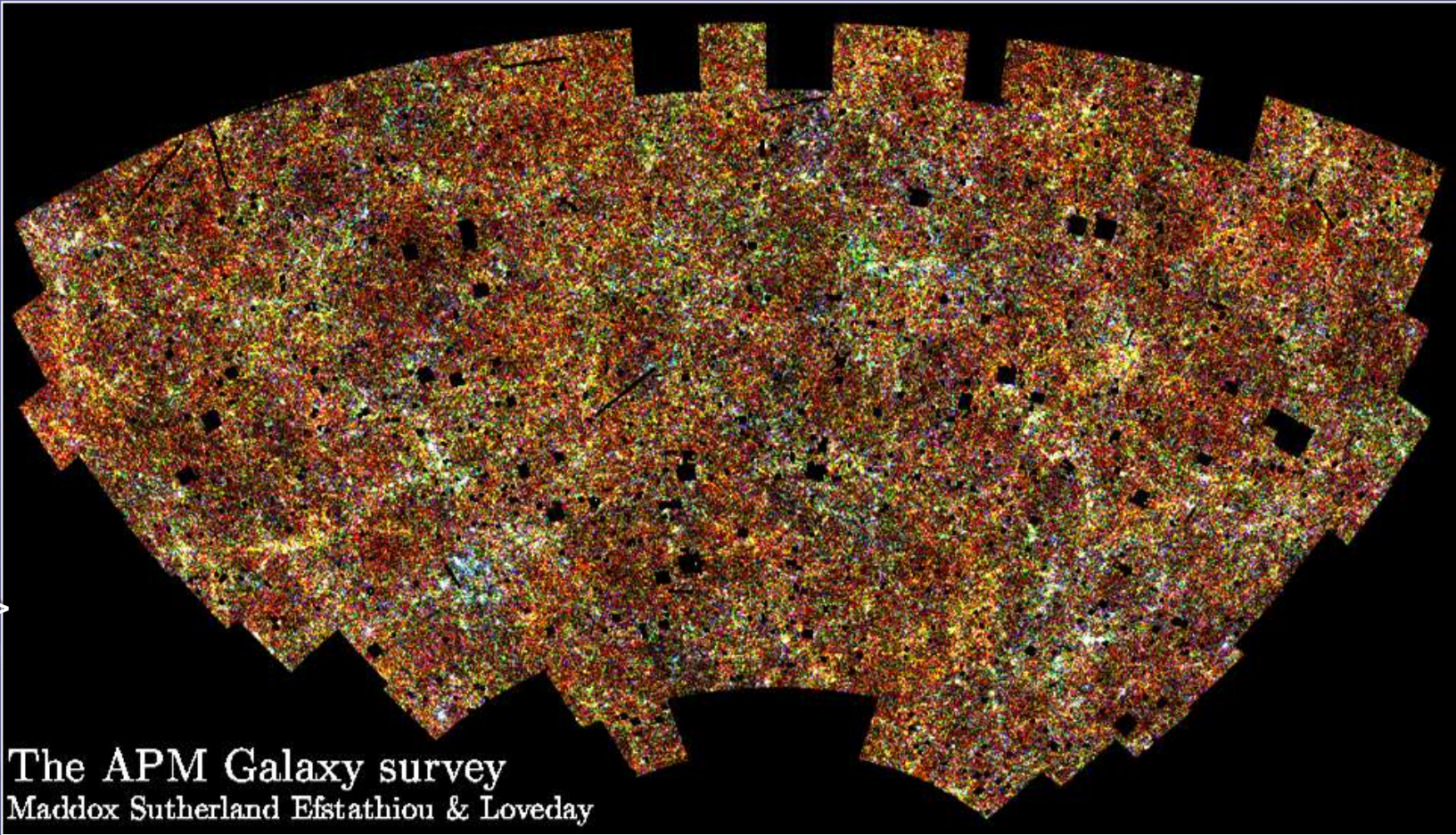
Total area
on sky ~
4300 deg²

250,000
galaxies in
total,

Mean
redshift $\langle z \rangle$
~ 0.1

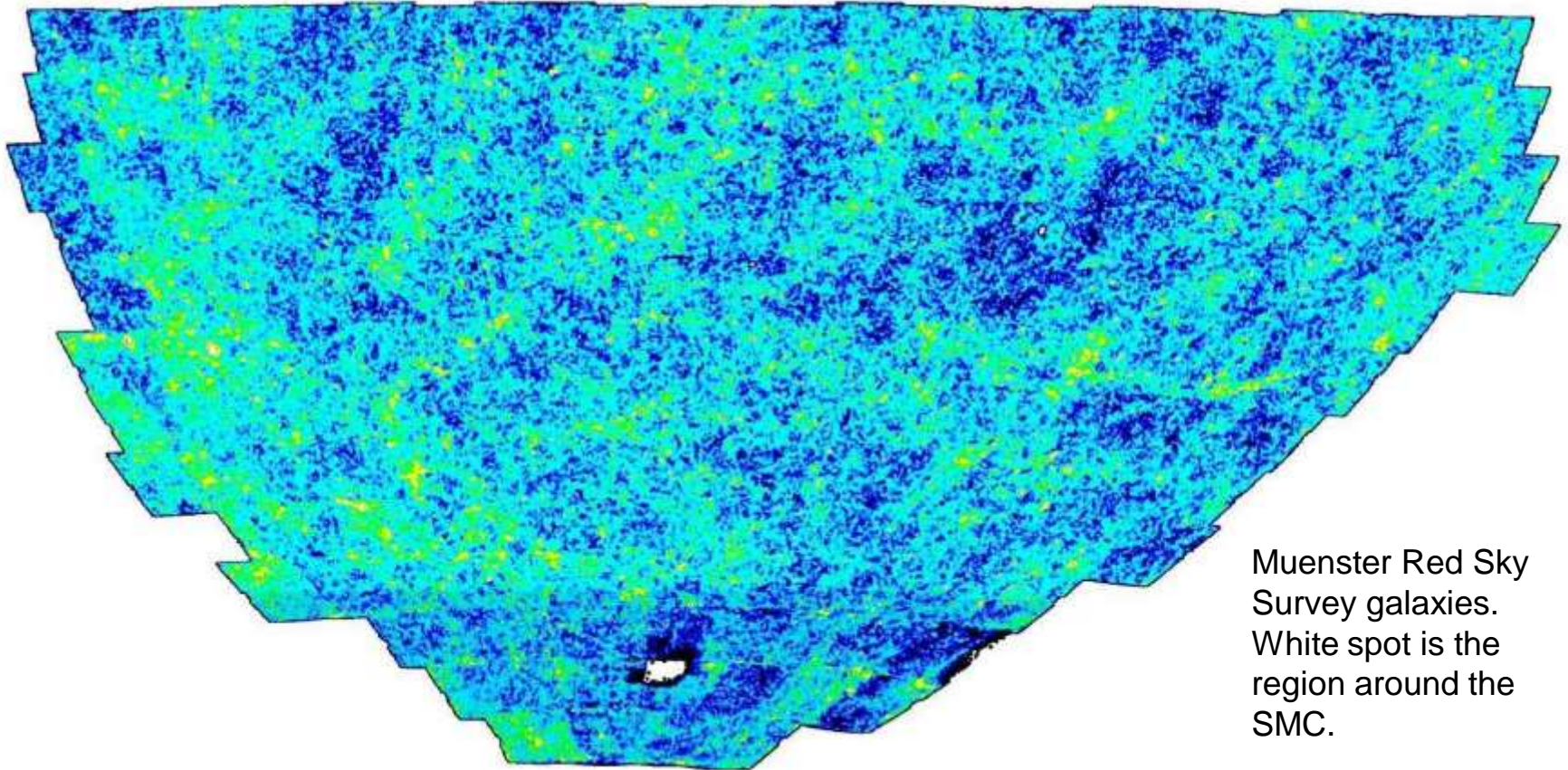
Blue

The APM Galaxy survey
Maddox Sutherland Efstathiou & Loveday

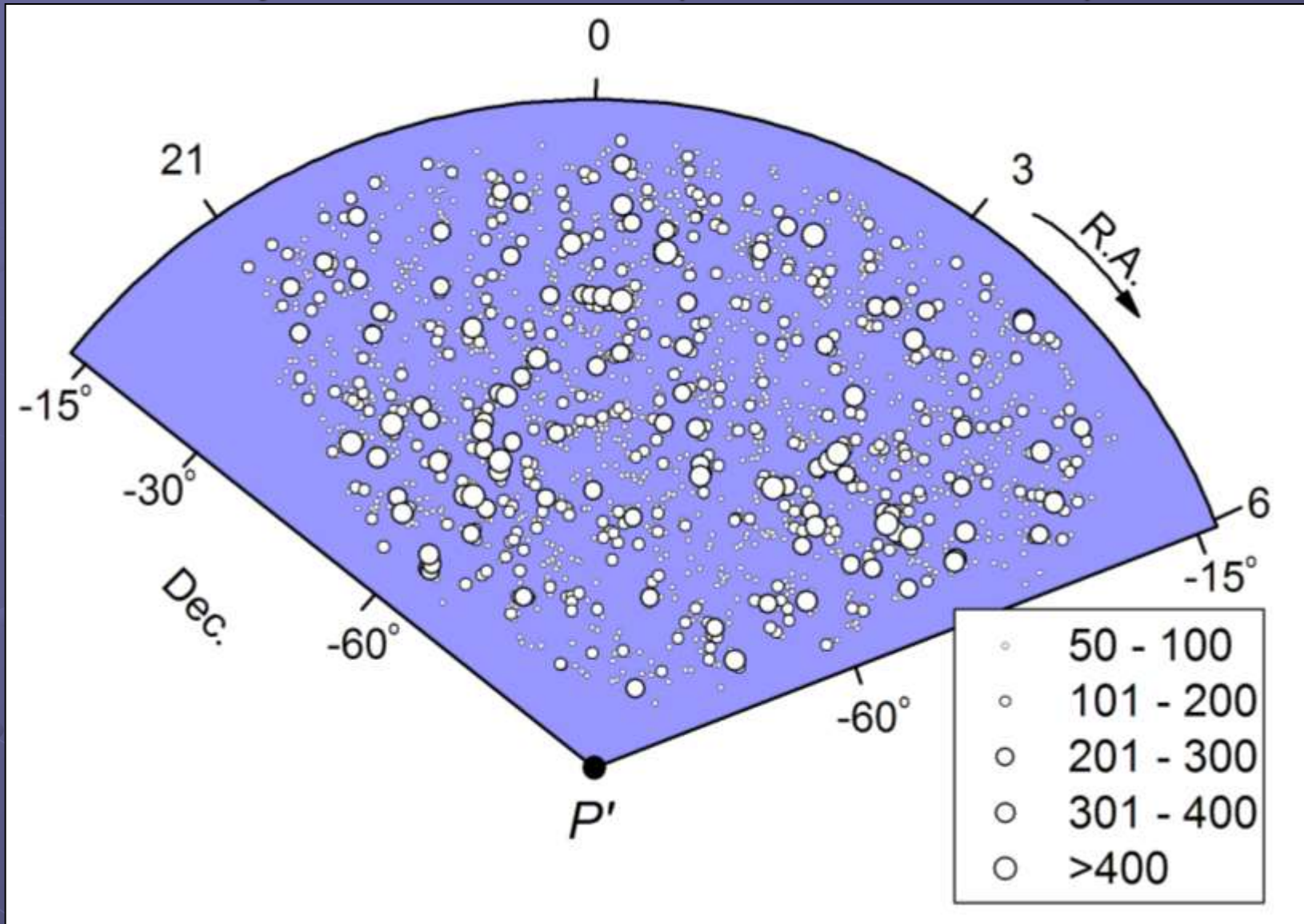


APM (Automatic Plate Measuring Machine). Main effort : scanning of UK Schmidt plates The first objective catalogue of clusters: Dalton G.B., Croft R.A.C., Efstathiou G. et al., [*Mon. Not. R. Astron. Soc.* **271** L47 \(1994\)](#)

Last 2D optical search for clusters: The Muenster Red Sky Survey. It covers an area of about 5000 deg² on the southern hemisphere. The catalogue includes 5.5 millions galaxies and is complete till to $r_F=18^m.3$ (Ungruhe, 1999). It's a result of scanning of 217 plates of Southern Sky Atlas R (ESO) by PDS 2020GM_{plus} and automated recognition of galaxies with careful control.

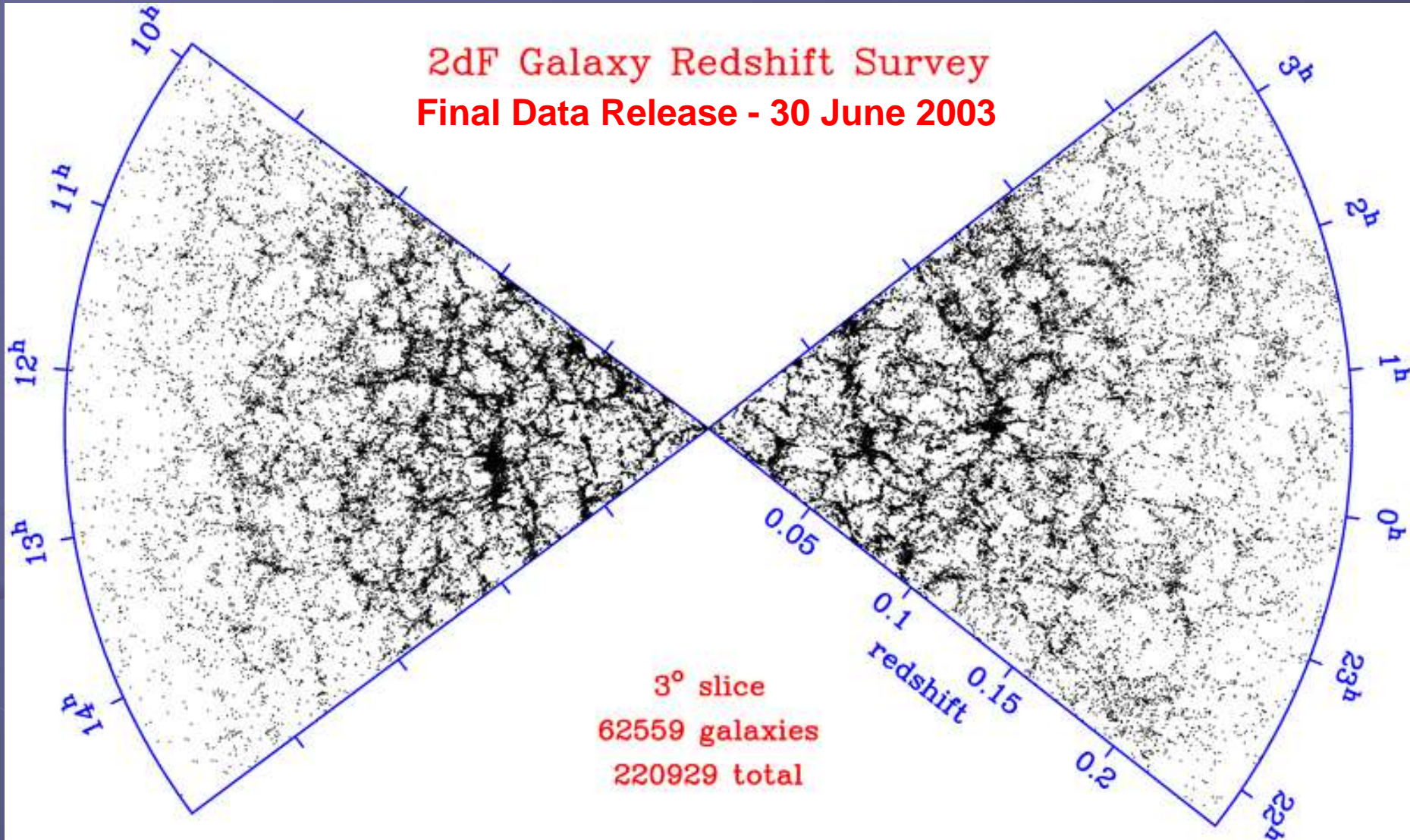


Galaxy clusters of MRSS (Panko & Flin, 2006)



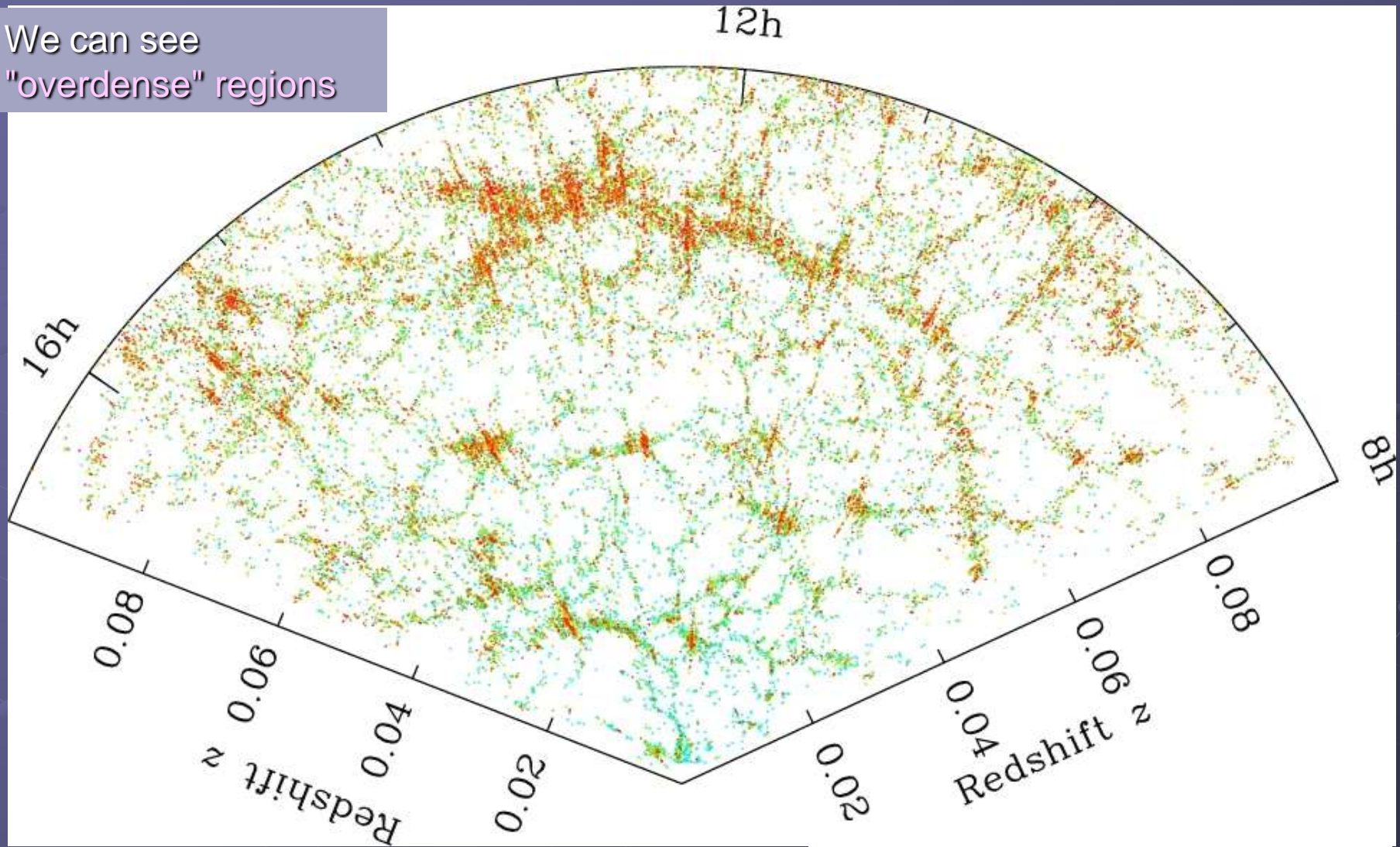
The data set allows to trace the development of galaxy clusters evolution changes.

**2dF Galaxy Redshift Survey
Final Data Release - 30 June 2003**



Galaxy distribution, SDSS

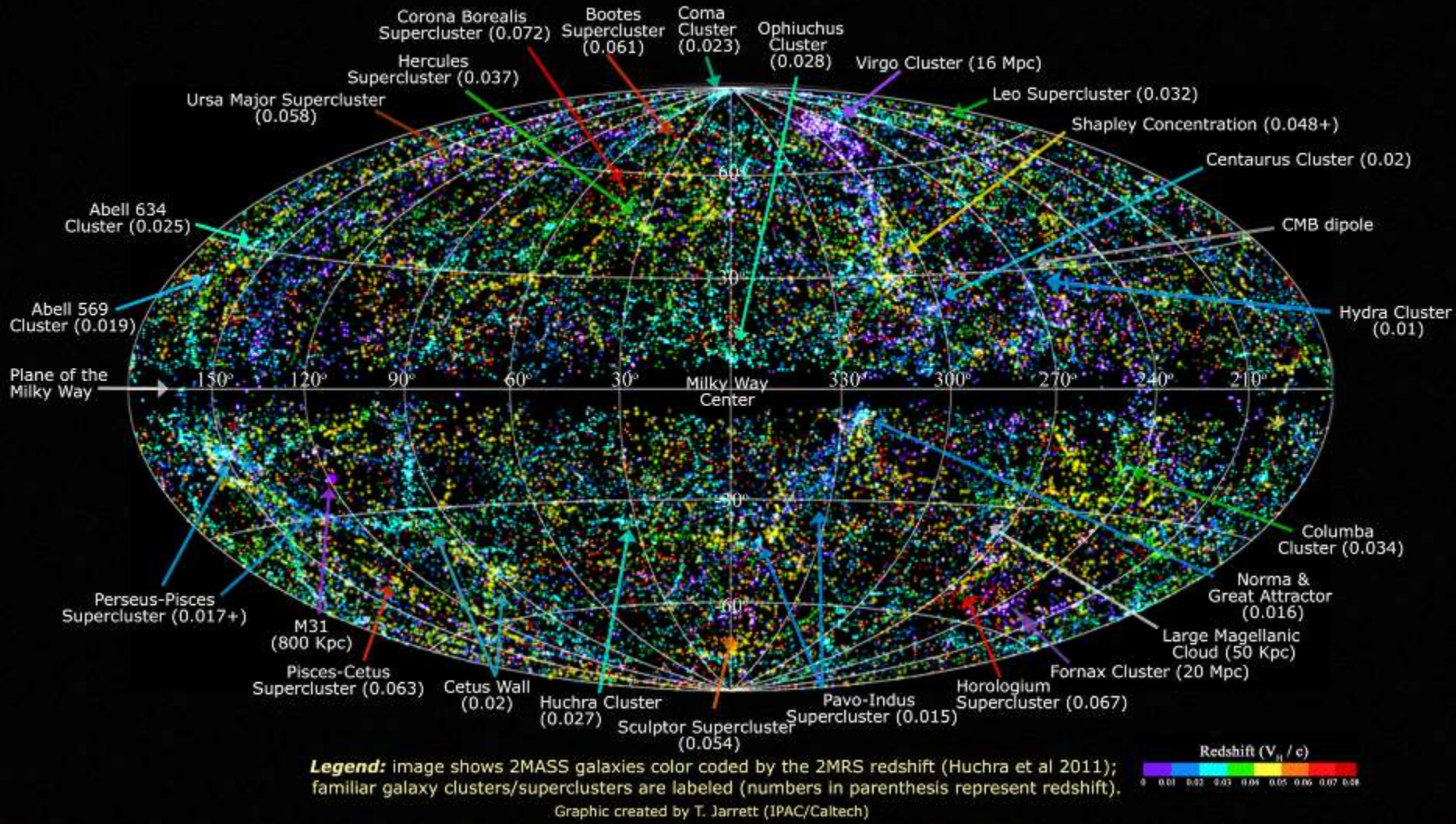
We can see
"overdense" regions



Credit: M. Blanton and the SDSS.

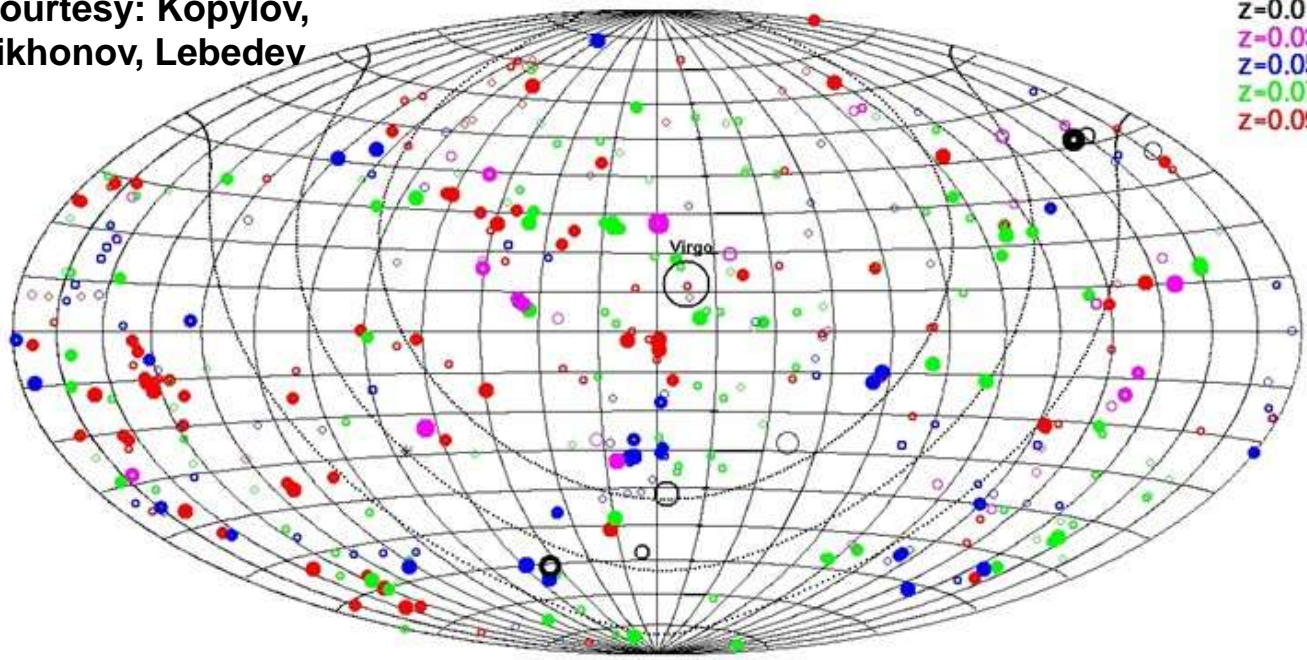
2MASS Redshift Survey

Courtesy: T.H. Jarrett (IPAC/SSC)



The Infrared Local Universe: 2MASS Redshift Survey. Measured redshifts of 44 000 galaxies. Colors coded by galaxy distances: violet ones are nearest ($0 < z < 0.01$), red ones are distant ($0.08 < z < 0.09$). Crook et al. in 2007 identified groups and clusters in the complete 11^m.25, mag limited 2MASS (*ApJ*, **655**, 790)§

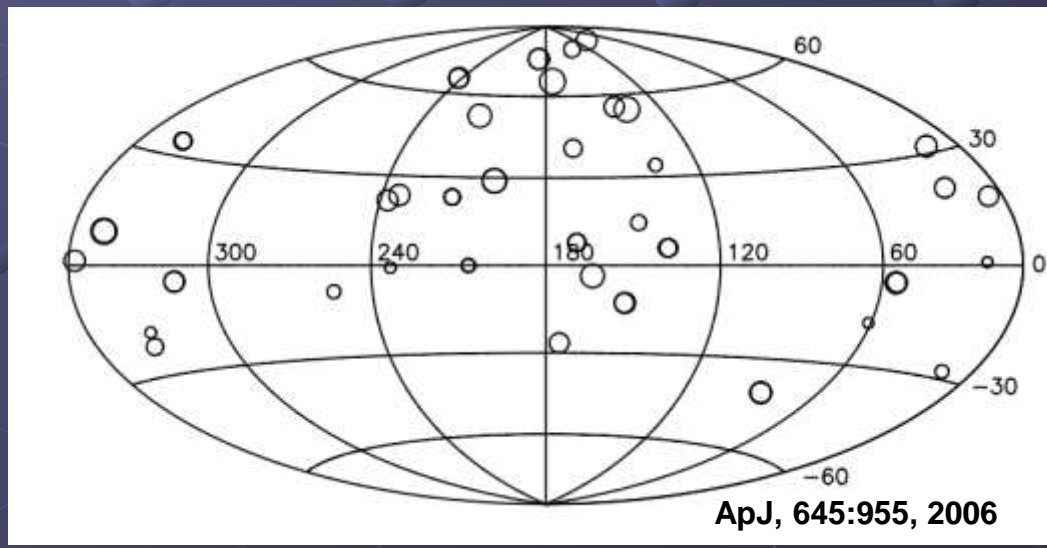
Courtesy: Kopylov,
Tikhonov, Lebedev



X-ray galaxy clusters

55 extended X-ray
Chandra sources.
Barkhouse et al

Nearest X-ray galaxy clusters,
collected data:
ROSAT All Sky: Fx(0.1-2.4 keV);
REFLEX (N = 186),
 Boringer et al., 2004;
eBCS (N = 108),
 Ebeling et al., 1998,
2002; NORAS (N=36),
 Boringer et al., 2000;
CIZA (N=70, |b|<20°),
 Ebeling et al., 2002, Kocevskiet al., 2006.



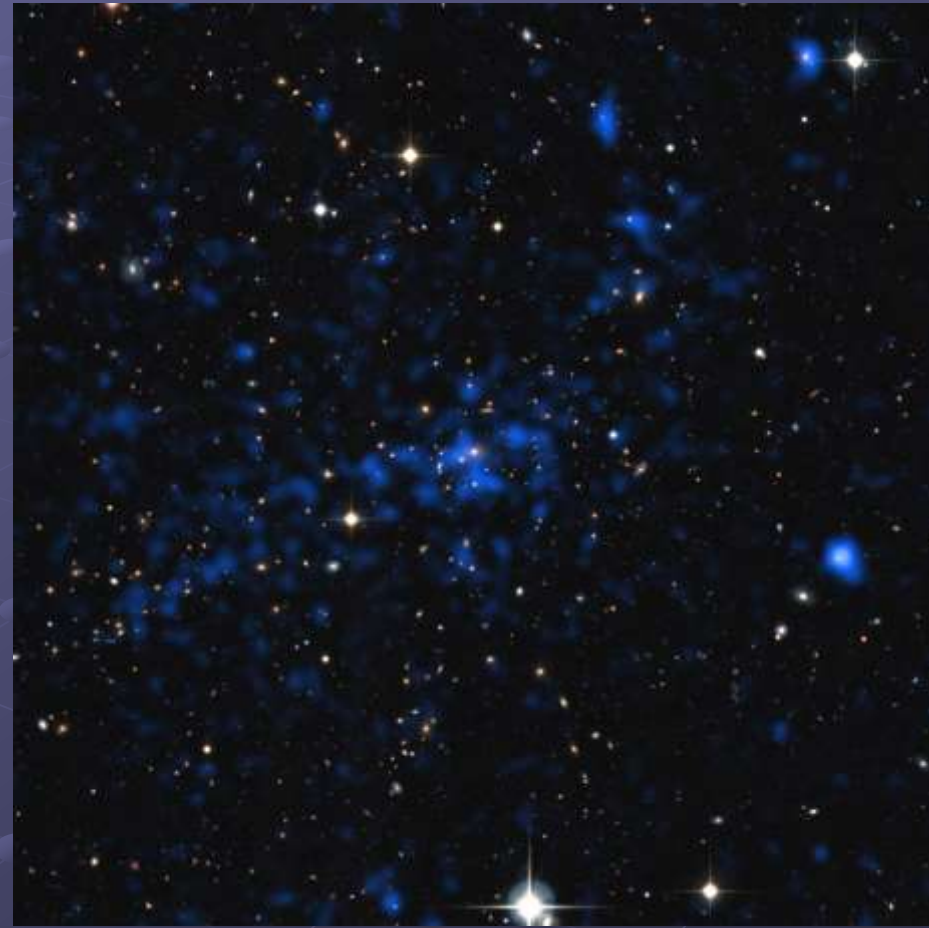
ApJ, 645:955, 2006

XXL Hunt for Galaxy Clusters

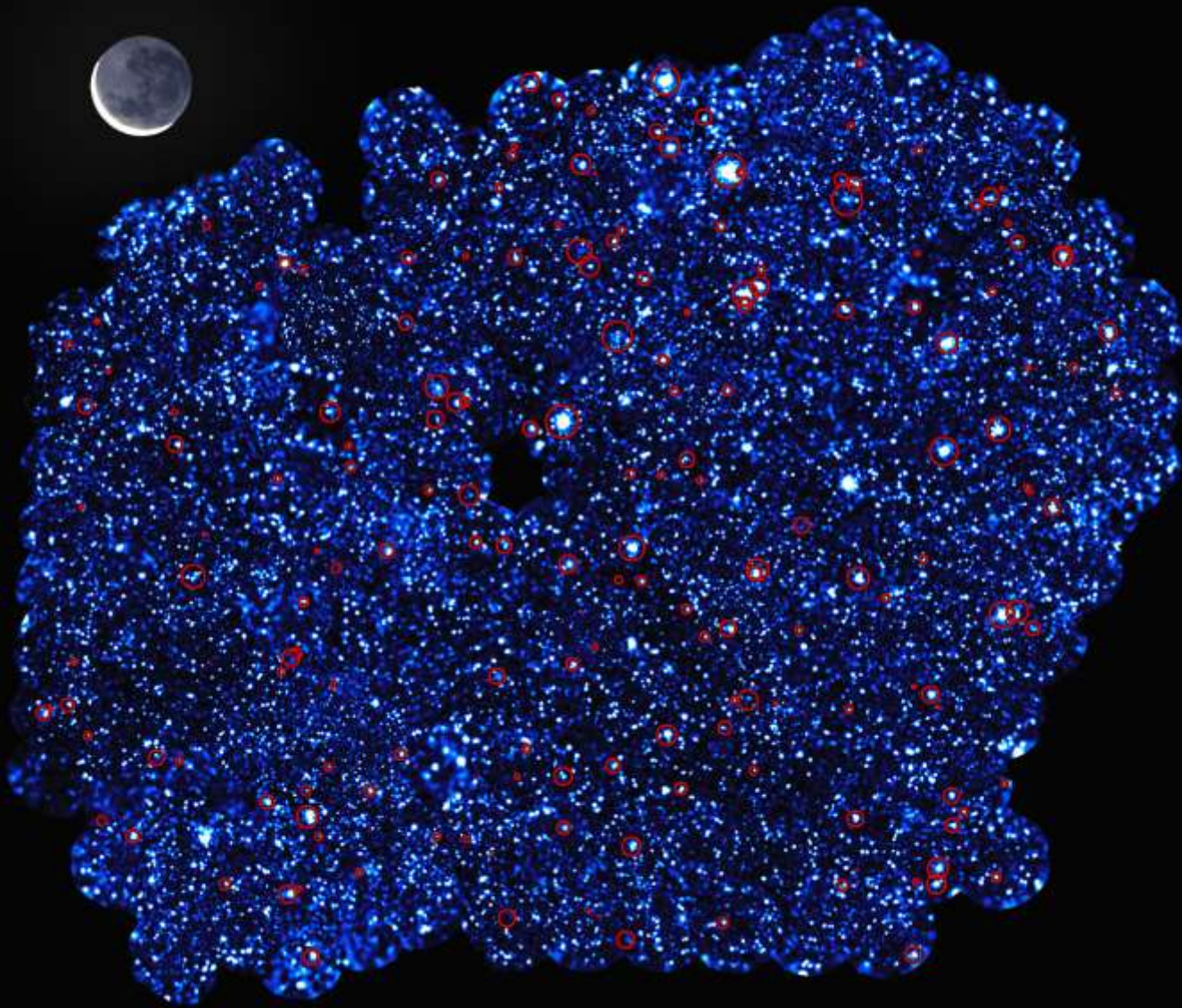
The XXL survey has combined archival data as well as new observations of galaxy clusters covering the wavelength range from $1 \times 10^{-4} \mu\text{m}$ (X-ray, observed with XMM) to more than 1 meter (observed with the Giant Metrewave Radio Telescope GMRT).



Visible light view of a distant galaxy cluster discovered in the XXL survey (PR Image eso1548c)



Composite of X-ray and visible light views of a distant cluster of galaxies (PR Image eso1548d)



XXL Hunt for Galaxy Clusters

Founded galaxy clusters with z from 0.05 to 1.05.

Observations by the VLT and the NTT complement those from other observatories across the globe and in space.

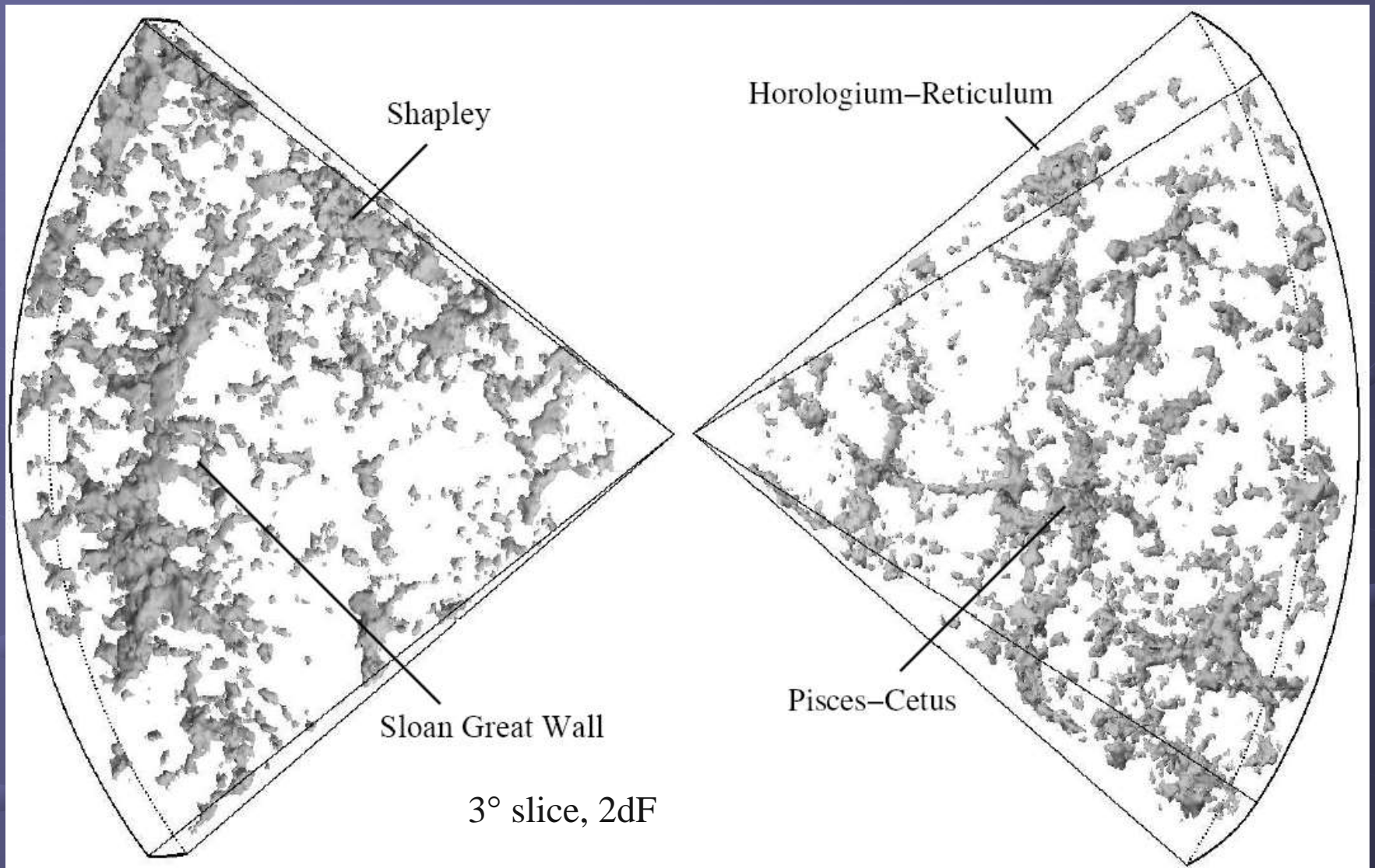
X-ray image of the XXL-South Field.

Clusters are noted as red circles.

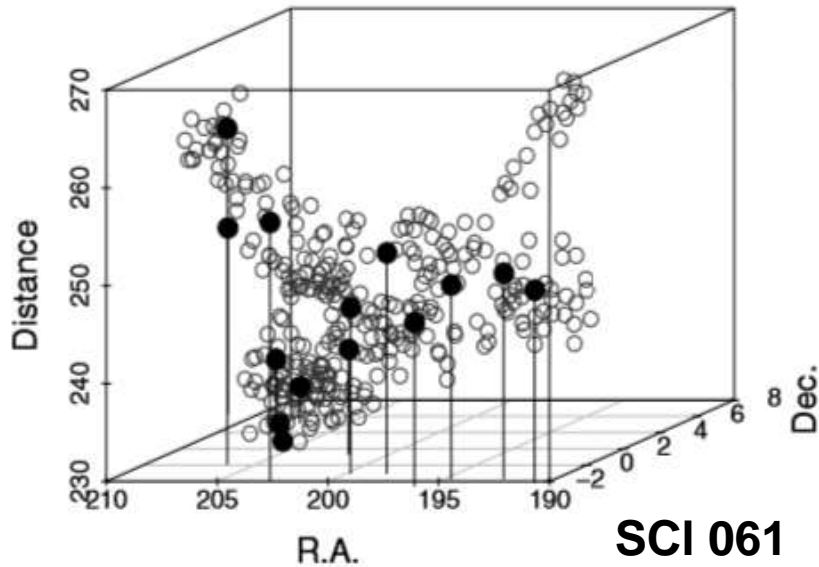
XXL-South Field: region of 25 deg^2 $23^{\text{h}}30^{\text{m}} -55^{\circ}00'$ (J2000)

Superclusters: Clusters of Clusters

Sizes: up to $50 h^{-1}$ Mpc, Masses of 10^{15} to $10^{16} M_{\odot}$

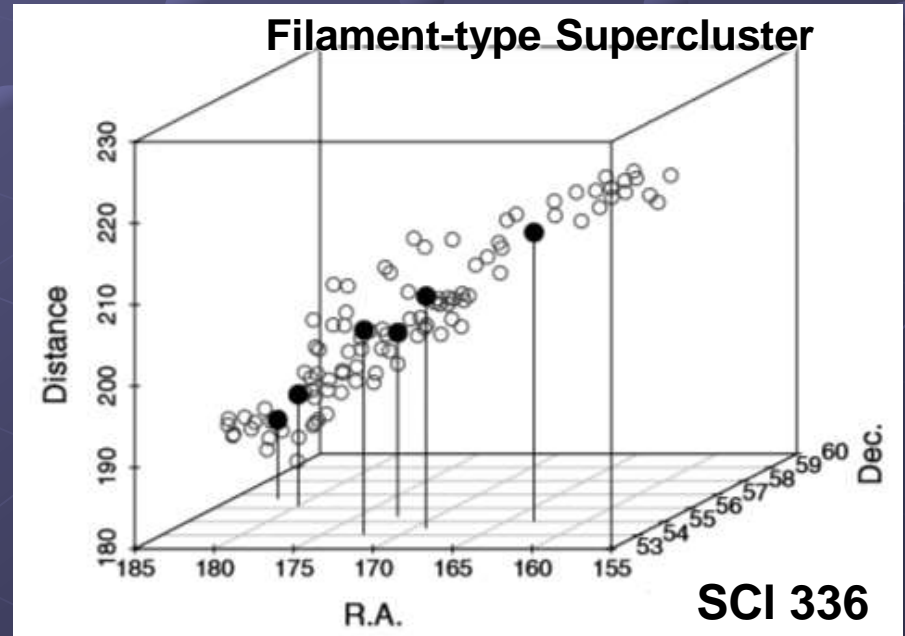
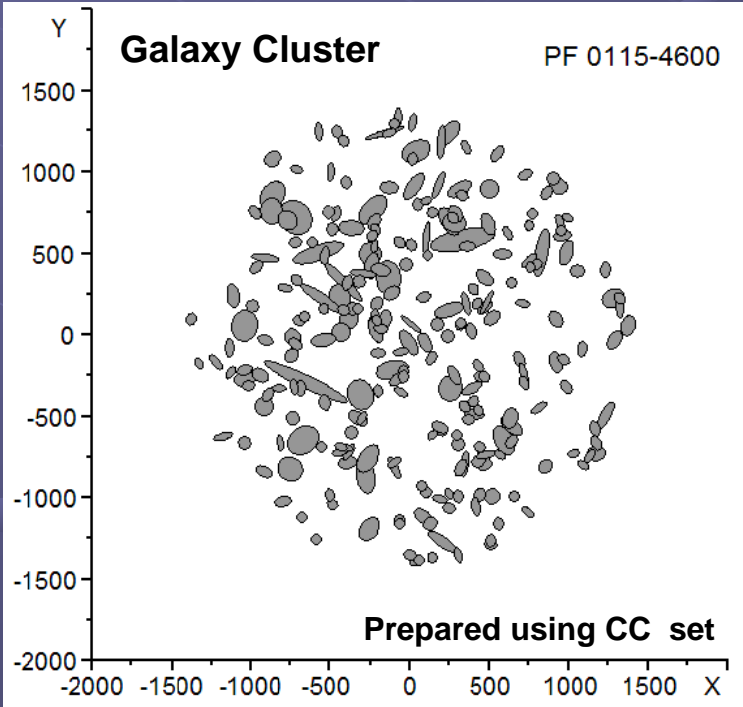


Spider-type Supercluster



Very rich superclusters founded in SDSS DR7. Filled circles show the location of rich groups and clusters with at least 30 member galaxies, empty circles show poorer groups.

M. Einasto et al.: Morphology of superclusters, A&A 532, A5, 2011



Methods of Identification of clusters

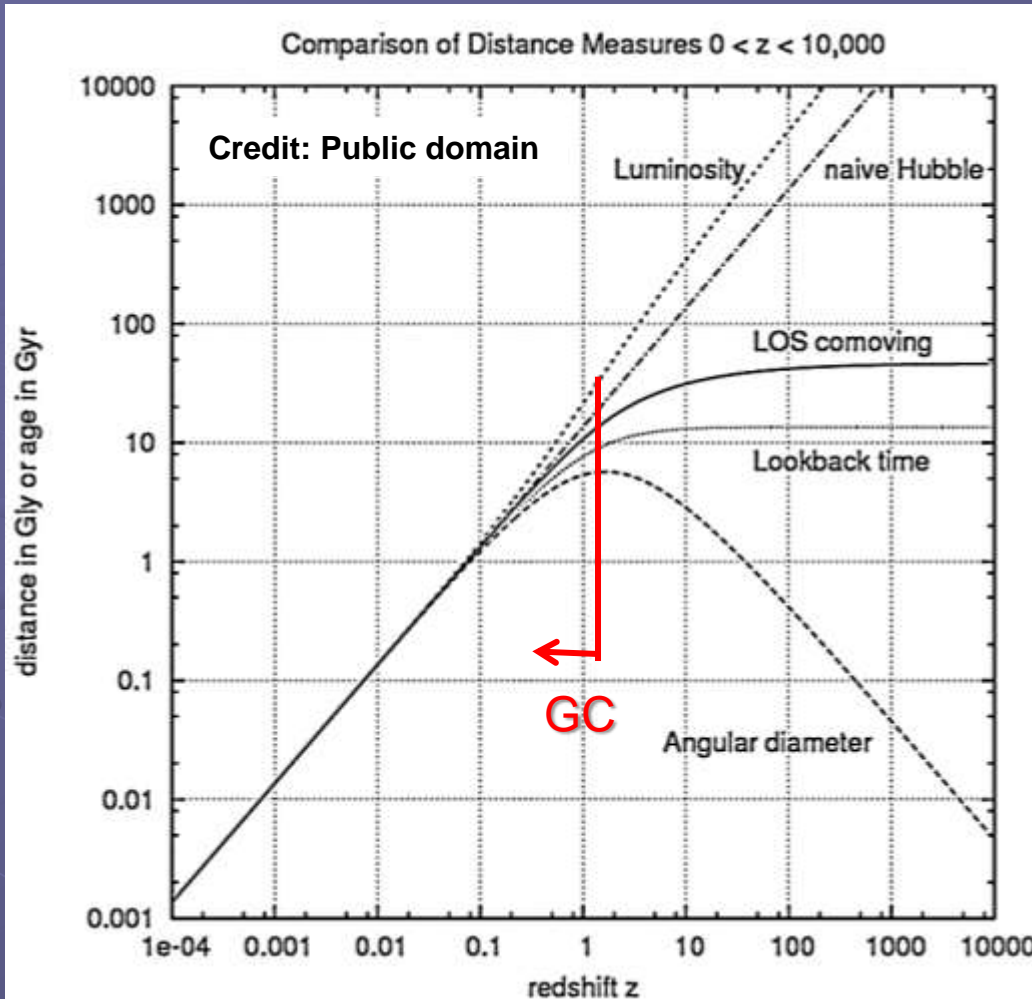
- Overdensity regions in surveys;
- X-ray Identification of rich clusters;
- SZ (Sunyaev-Zeldovich) effect;
- Weak Gravitational Lensing;
- Color Search for Red Galaxies.

And how far are they?

See, for example, **DISTANCE MEASURES IN COSMOLOGY** by David W. Hogg

https://ned.ipac.caltech.edu/level5/Hogg/Hogg_contents.html

What does mean "to measure distance"? How fare is it?



$H_0 = 72 \text{ km/s/Mpc}$, $\Omega_\Lambda = 0.732$, $\Omega_{\text{matter}} = 0.266$,
 $\Omega_{\text{radiation}} = 0.266/3454$ and, and Ω_k chosen so
 that the sum of Omega parameters is one.

The proper distance roughly corresponds to where a distant object would be at a specific moment of cosmological time, which can change over time due to the expansion of the universe.

The comoving distance between fundamental observers (moving with the Hubble flow) does not change with time.

Comoving distance and proper distance are defined to be equal at the present time (the scale factor is equal to 1. At other times, the scale factor differs from 1. The Universe's expansion results in the proper distance changing, while the comoving distance is unchanged by this expansion.

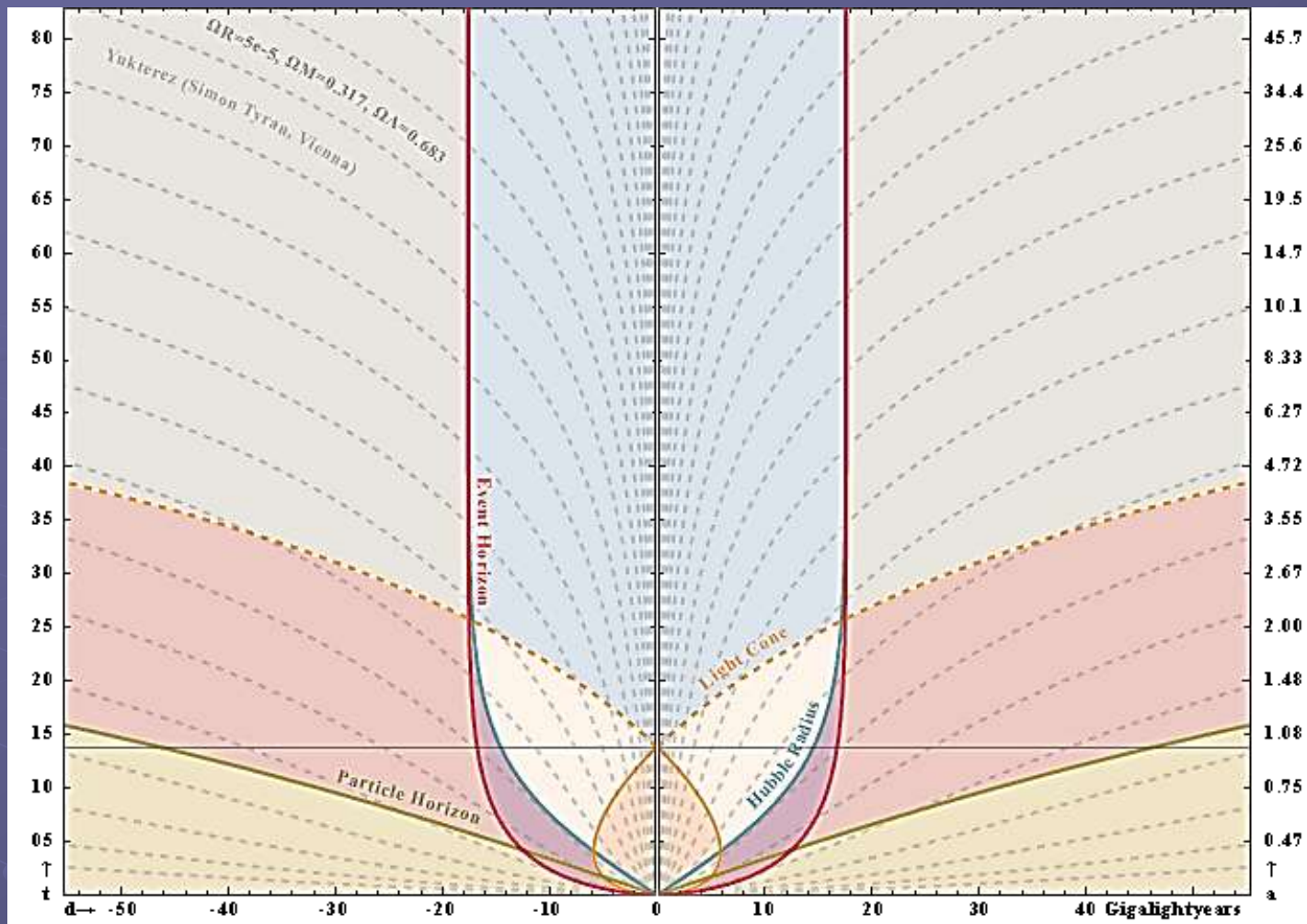
Comoving distance on-line calculator:

The screenshot shows a web browser window with the address bar containing the URL `www.wolframalpha.com/widgets/view.jsp?id=453fadbd8a1a3af50a9df4df899537b5`. The browser's address bar also shows several tabs: "FaceNEWS -- in...", "Переводчик Google", "Вільногірськ! ***", "Моделирование", "Учебники по аст", and "Ресурси, со".

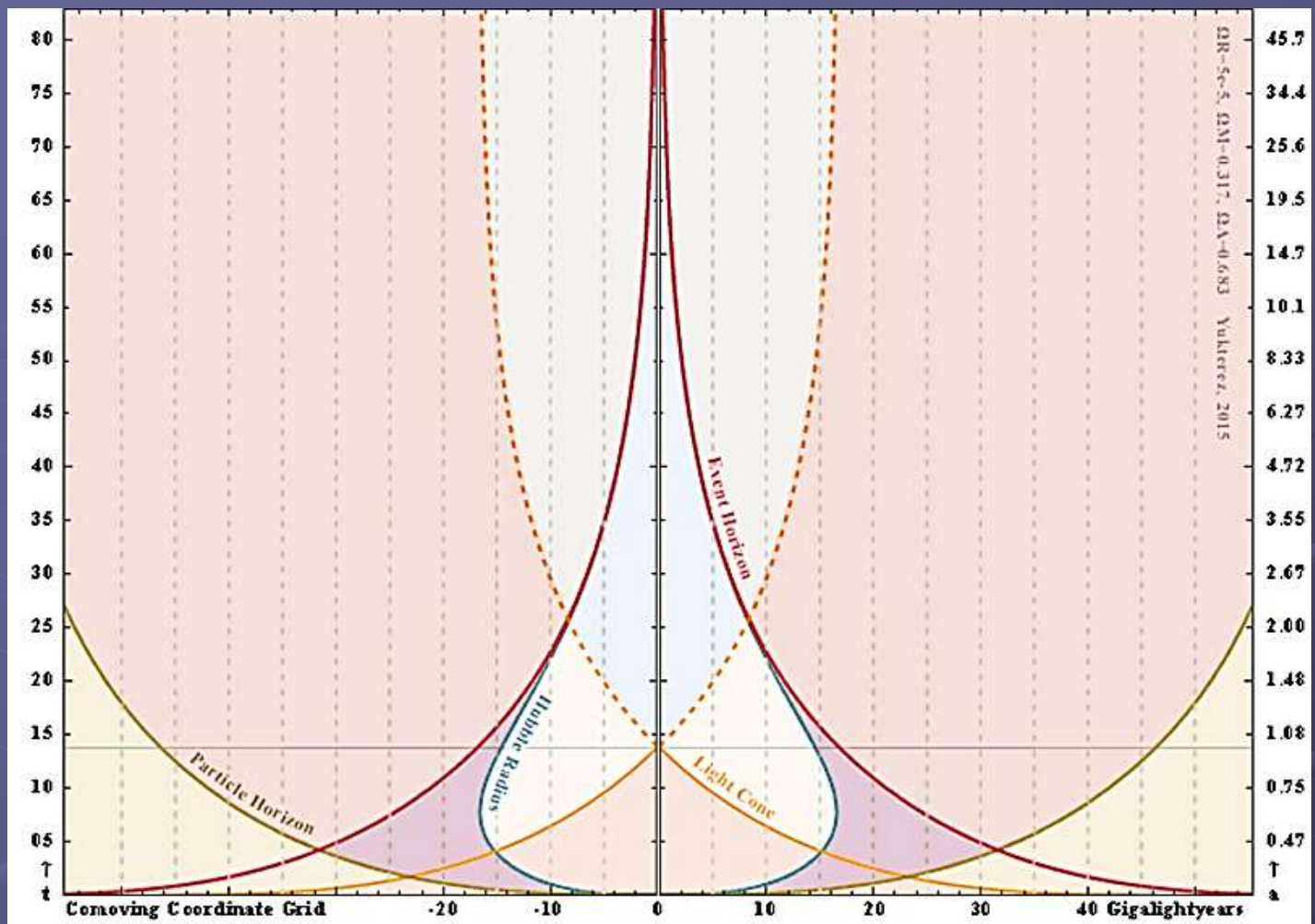
The main content area features a widget titled "Comoving Distance in Mpc from redshift (stand)". Below the title is a "Privacy Policy" link. The widget itself is a red-bordered box with a "BETA" badge in the top right corner. It contains the following fields and controls:

- Hubble constant (km/s/Mpc):
- Omega Matter:
- Redshift:
- A red "Submit" button.
- WolframAlpha logo and icons in the bottom left and right corners.

Below the widget, a grey footer area contains the text: "Added Aug 1, 2010 by aristarchos in Astronomy" and "Comoving distance in Mpc from redshift assuming a flat Lambda CDM model. ($\Omega_{\Lambda} = 1 - \Omega_{\text{Matter}}$).



Expansion of the universe, proper distances diagram. X-axis: Proper distance in billion light years. Y-axis: time since Big Bang in billions of years, scale factor a . Shown are the Particle Horizon (brown), Event Horizon (red), Hubble Radius (blue). The horizontal black line describes the present. Past and future light cones (orange) are animated. Dashed grey lines are lines of constant comoving distances (i.e. the Hubble flow).



Expansion of the universe, comoving coordinate grid. X-axis: Comoving distance in billion light years. Y-axes: time since Big Bang in billions of years, scale factor a . Shown are the Particle Horizon (brown), Event Horizon (red), Hubble Radius (blue). The horizontal black line describes the present. Past and future light cones (orange) are animated. Dashed grey lines are lines of constant comoving distances (i.e. the Hubble flow).

Methods of Identification of clusters

X-ray Identification of rich clusters

- Rich clusters with deep potentials have hot gas
- X-ray emission is an effective way to find relaxed clusters
- Since emissivity $\sim n^2$, we have \sim no foreground X-ray emission (though smooth X-ray background)
- Problems of spurious identification from superposition is **greatly reduced** compared to optical surveys
- At high redshifts, this is increasingly important
- X-ray surveys may be the best way to identify (rich) high-z clusters
- Several surveys currently exist: EMSS (Einstein Medium Sensitivity Survey: serendipitous, 800 deg², $z \sim 0.05 - 0.55$); RDCS (ROSAT Deep Cluster Survey: serendipitous, 100 deg², $z \sim 1$); RASS (ROSAT All Sky Survey); XCS (XMM cluster survey); Chandra.

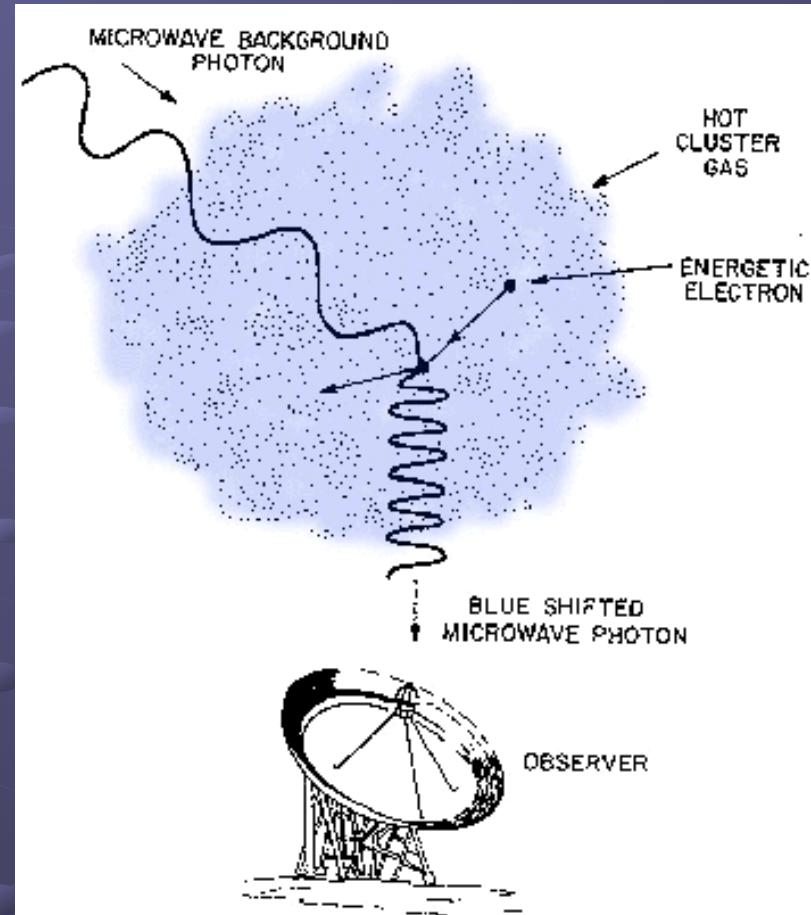
The number of X-ray detected clusters is around 5 000 now with \sim 500 with measured temperatures and Fe abundances.

Other Methods of Identification of clusters

- **SZ (Sunyaev-Zeldovich) effect :**
Cosmic microwave background (CMB) photons passing through hot intracluster hot gas have a ~1% chance of inverse-Compton scattering off the plasma's energetic electrons, causing a small (~ 1 mK) distortion in the CMB spectrum. So, look for brightening/dimming of CMB at mm-wavelengths. Promising for detecting high-z clusters SPT, **PLANCK!**

One of more massive distant galaxy cluster SPT-CL J0546-5345 was found using SZ effect and spectroscopically confirmed by Brodwin et al. (*ApJ*, 721, 90, 2010).

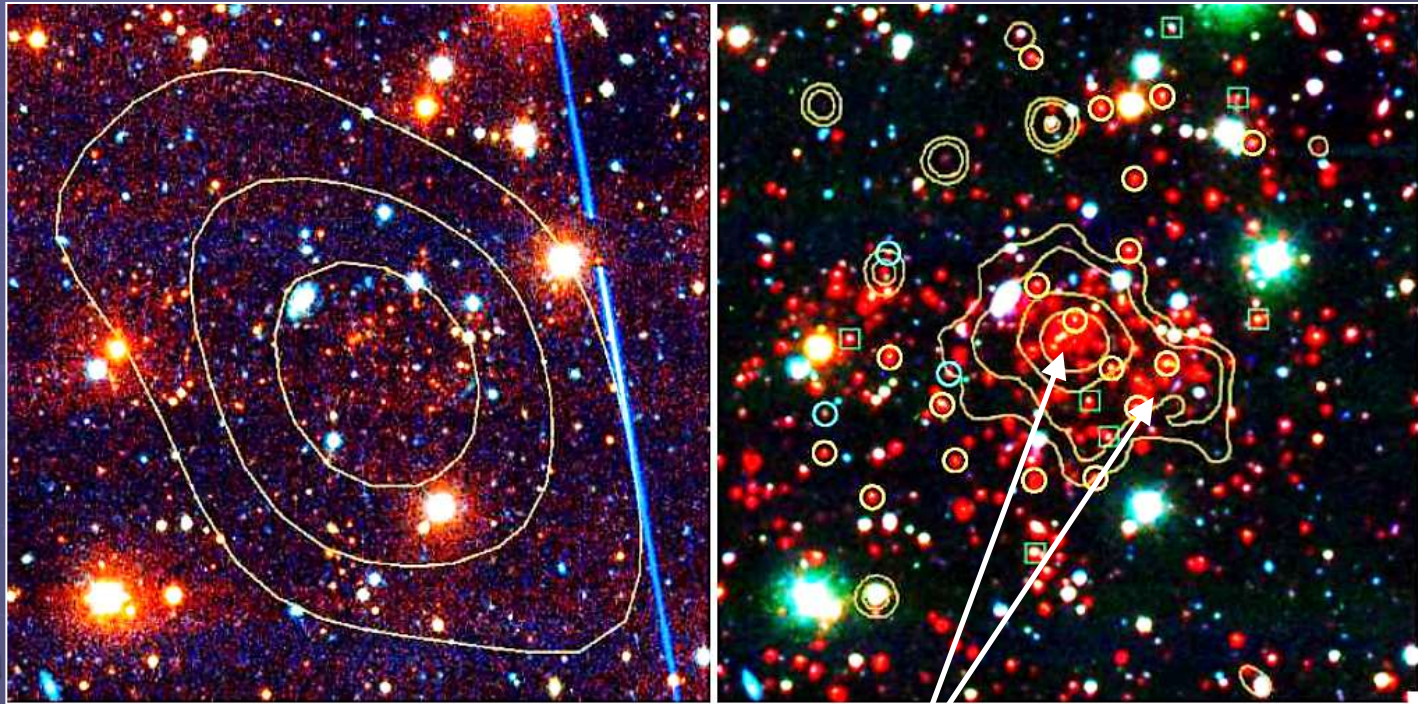
It places in Pictor; $z = 1.067$;
the velocity dispersion is 1179^{+232}_{-167} km/s;
best-estimate mass of $M = (7.95 \pm 0.92) \times 10^{14} M_{\odot}$.



Images of SPT-CL J0546-5345.

Left: Optical $4' \times 4'$ color (*grz*) with SZE significance contours overlaid (S/N = 2, 4, and 6).

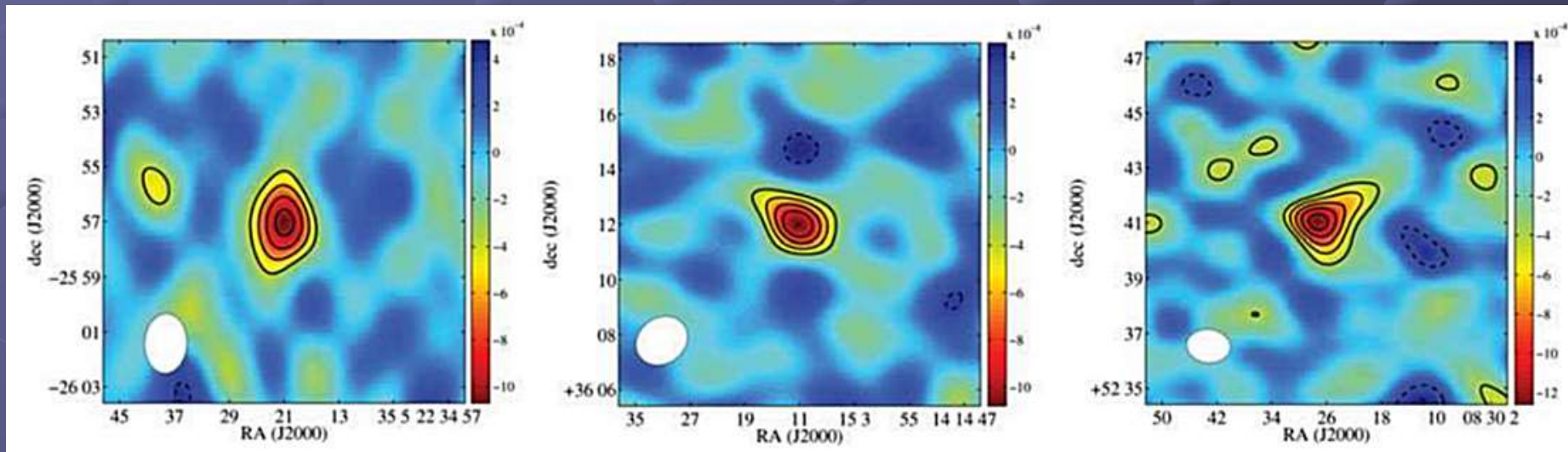
Right: False color optical (*ri*) + IRAC ($3.6 \mu m$) image of SPT-CL J0546-5345, with Chandra X-ray contours overlaid (0.25, 0.4, 0.85 and 1.6 counts per $2'' \times 2''$ pixel per 55.6 ks in the 0.5-2 keV band)



Note, Chandra is able to resolve substructures, which may be evidence of a possible merger. Spectroscopic early-type (late-type) members are indicated with yellow (cyan) circles. Green squares show the spectroscopic non-members.

Images of clusters with significant SZE detections. From left to right, XMMU J2235-2557, CI J1415.1+3612, and 2XMM J083026.2+524133, with the color scale given in Jy beam^{-1} . The contours start at 2σ and spaced at 1σ . The white ellipse represents the half-power point of the elliptical 2D Gaussian function that approximates the main lobe of the synthesized beam.

X-ray and SZE observations of galaxy clusters provide a unique method to measure distances to distant galaxy clusters.

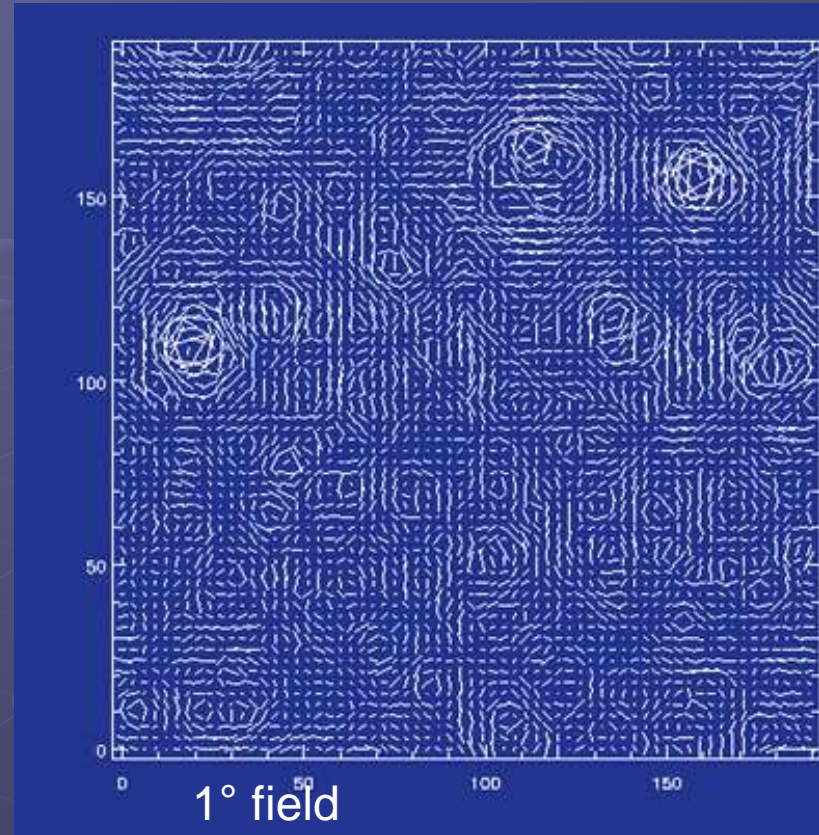
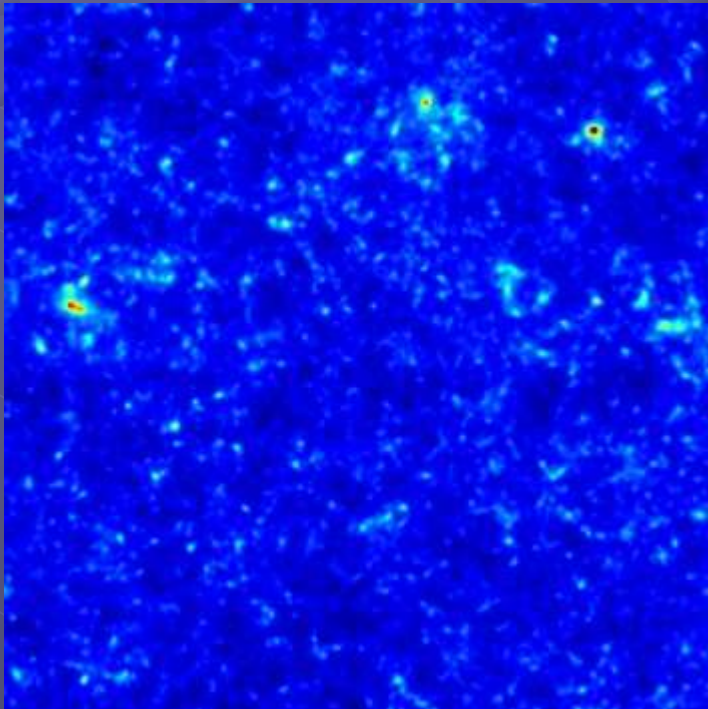


M. Bonamente et al. in: Advancing the Physics of Cosmic Distances
Proceedings IAU Symposium No. 289, 339, 2012. Richard de Grijs, ed.

Other Methods of Identification of clusters

Weak Gravitational Lensing :

Faint background galaxies suffer slight distortion by matter along the line of sight. Intervening clusters give slight azimuthal image elongation. For big sample of galaxies it is statistically detectable and allows mapping of intervening mass distribution.



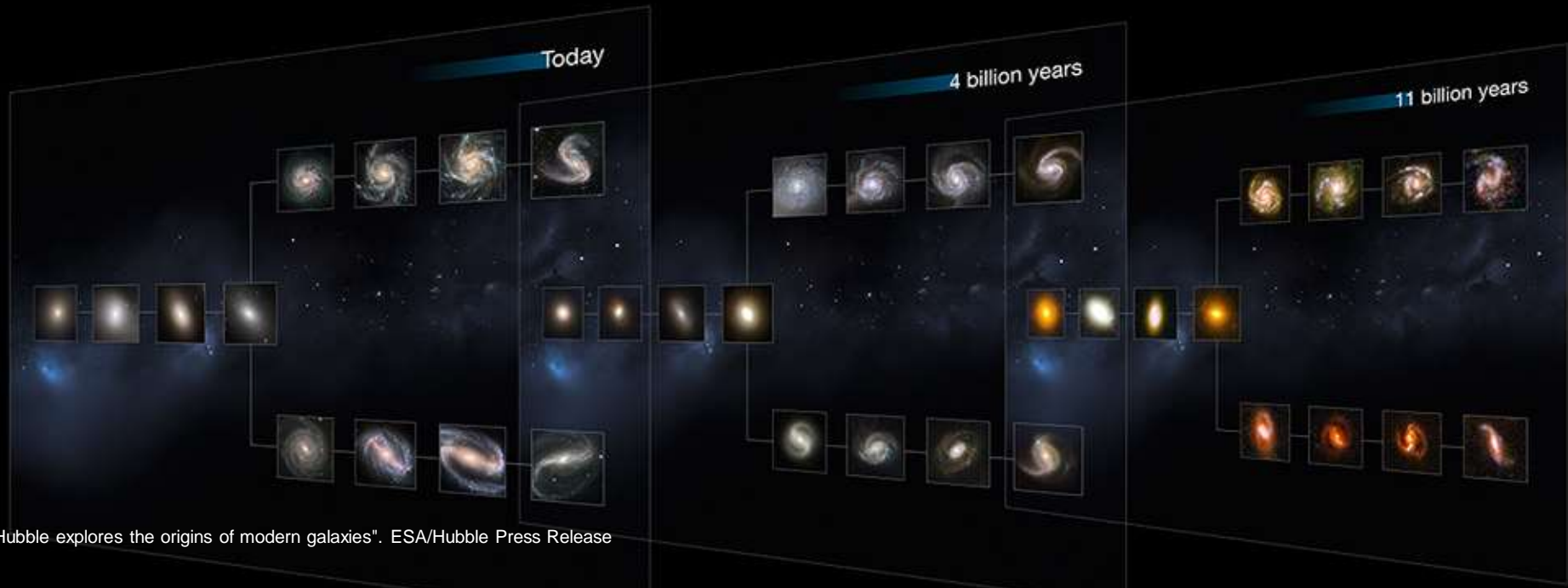
Weak lensing simulation by B. Jain, U. Seljak, and S. White (*AJ*, **530**, 547, 2000).

Other Methods of Identification of clusters

● Color Search for Red Galaxies:

Elliptical (Red) galaxies formed very early so concentrations of faint red objects should yield high-z clusters. Redshift modifies colors, so good color information should also yield approximate redshift.

Need: deep multicolor surveys.



"Hubble explores the origins of modern galaxies". ESA/Hubble Press Release

The four principal constituents of clusters include:

- Galaxies;
- Intracluster Stars;
- Hot Gas;
- Dark Matter.

Ongoing: heierarchical assembly.

Clusters continue to grow (and form), even today.

The physics of the principal constituents of clusters

Galaxies

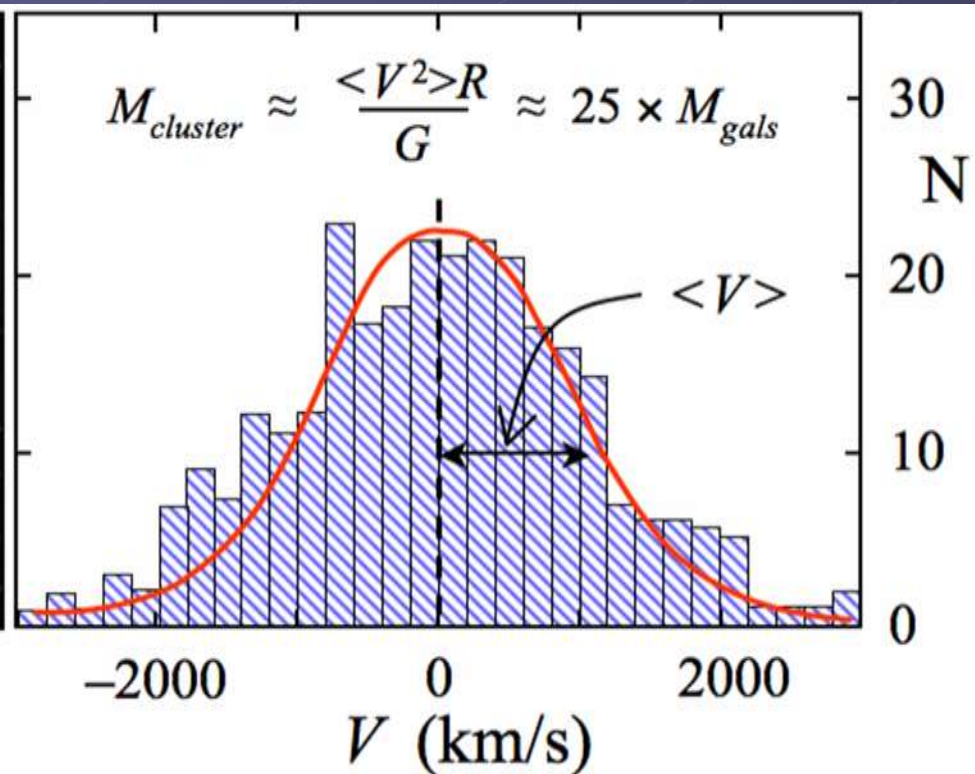
$\sim 10^2$ large galaxies;

$> 10^3$ total galaxies

Typical speeds $\sim 10^3$ km/s – allows to estimate the mass of cluster



Coma cluster (central part)



The ensemble of thousands galaxies inside the cluster one can study statistically:
luminosity function, mass function

Luminosity Functions

The luminosity function (LF) of galaxies in a cluster gives the number distribution of the luminosities of the galaxies. The integrated luminosity function $N(L)$ is the number of galaxies with luminosities greater than L , while the differential $LF(L)dL$ is the number of galaxies with luminosities in the range L to $L + dL$. Obviously, $n(L) \equiv -dN(L)/dL$. LF are often defined in terms of galaxy magnitudes $m \sim -2.5 \log_{10}(L)$; and $N(\leq m)$ is the number of galaxies in a cluster brighter than magnitude m .

Sure, LF depends from Hubble mix in cluster.

The Luminosity function contains information about :

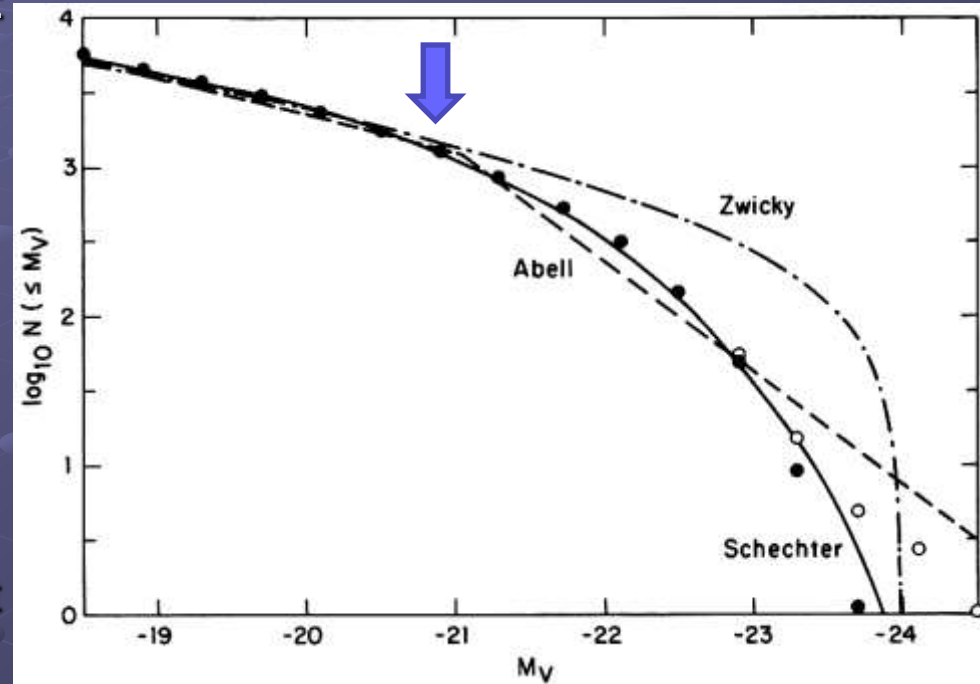
- ✓ primordial density fluctuations;
- ✓ processes that destroy/create galaxies;
- ✓ processes that change one type of galaxy into another (eg mergers, stripping);
- ✓ processes that transform mass into light.

Real LF describes by Schechter function:

$$N(L) = N^* \Gamma(\alpha, L/L^*),$$

where L^* is a characteristic luminosity, $N^* \Gamma(\alpha, 1)$, is the number of galaxies with $L > L^*$, $\Gamma(\alpha, x)$, is the incomplete gamma function, and $\alpha = 5/4$ for the faint end slope (Schechter, 1976).

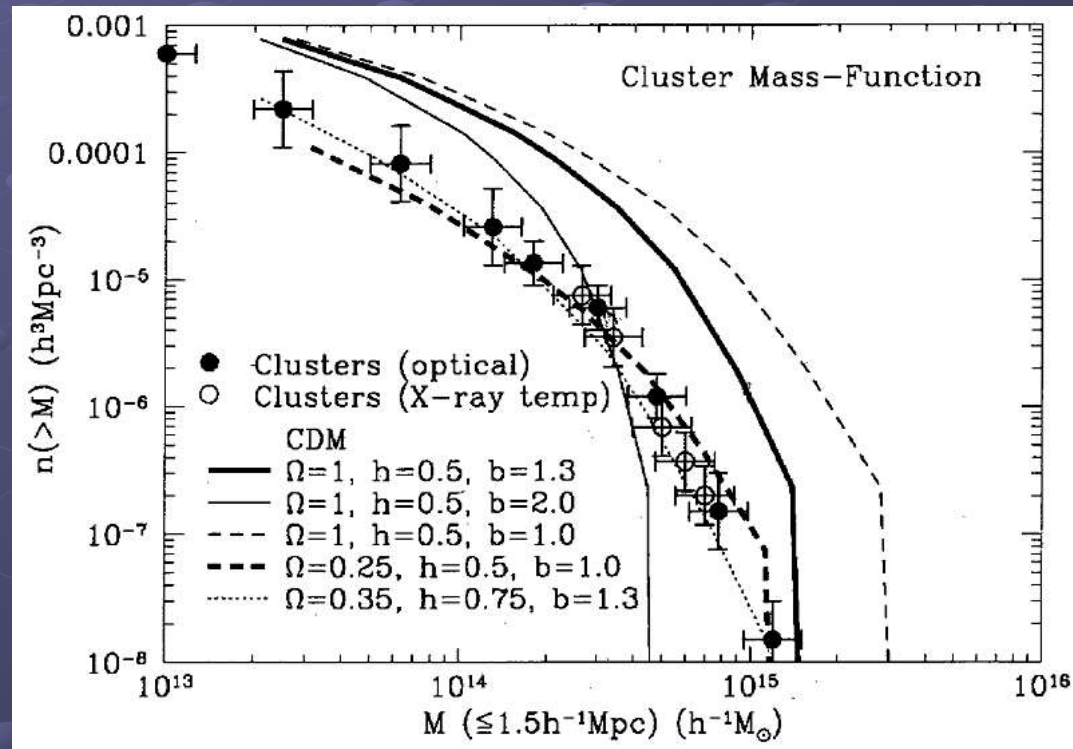
The Schechter function fits the observed distribution reasonably well from the faint to the bright end, as long as the very brightest galaxies, the cD galaxies, are excluded.



Mass Functions

The observed mass function (MF), $n(> M)$ of clusters of galaxies, which describes the number density of clusters above a threshold mass M , can be used as a critical test of theories of structure formation in the Universe. The richest, most massive clusters are thought to form from rare high peaks in the initial mass-density fluctuations; poorer clusters and groups form from smaller, more common fluctuations.

The observed cluster mass function in comparison with expectations from different CDM cosmologies using large-scale simulations (Bahcall and Cen, 1992). Observed MF is indeed a powerful discriminant among models. A low-density CDM model, with $\Omega \sim 0.2-0.3$ (with or without a cosmological constant), appears to fit well the observed cluster MF .



Bahcall, N. A., & Cen, R. 1992, *ApJ*, **398**, L81

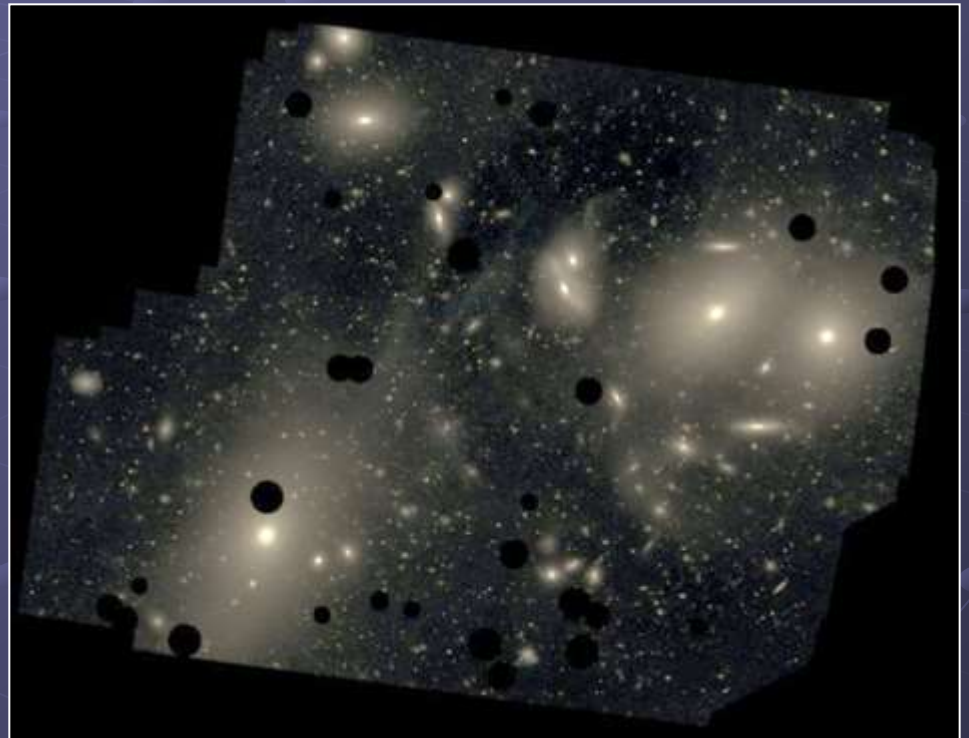
The physics of the principal constituents of clusters

● Intracluster Stars

very faint ($\sim 1\%$ sky) diffuse light (distinct from cD halo light) comprises 10-50% total galaxy light (in rich clusters; much less in poor clusters) probably tidally stripped stars;



Wide angle view of most of the Virgo cluster from the DSS.



Deep image of Virgo by Chris Mihos et al, (2005) by Burrell Schmidt (bright stars removed). See also M. Doherty et al.: The M87 Halo and the Diffuse Light in the Virgo Core. A&A, 2009

The physics of the principal constituents of clusters

- Hot Gas -- Hydrostatic equilibrium

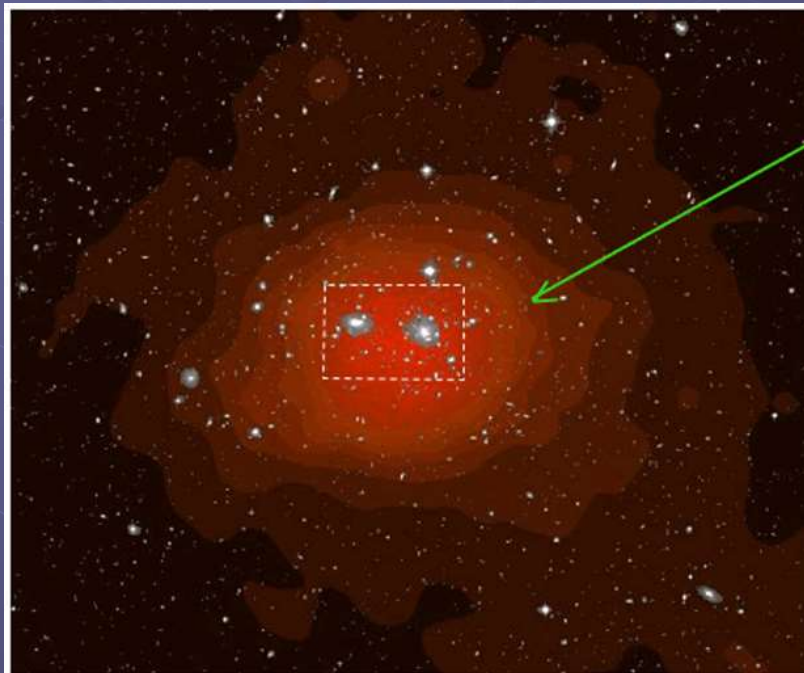
$T \sim 10^7\text{-}8\text{K}$ (X-ray emitter)

$n \sim 10^{-3} \text{ cm}^{-3}$

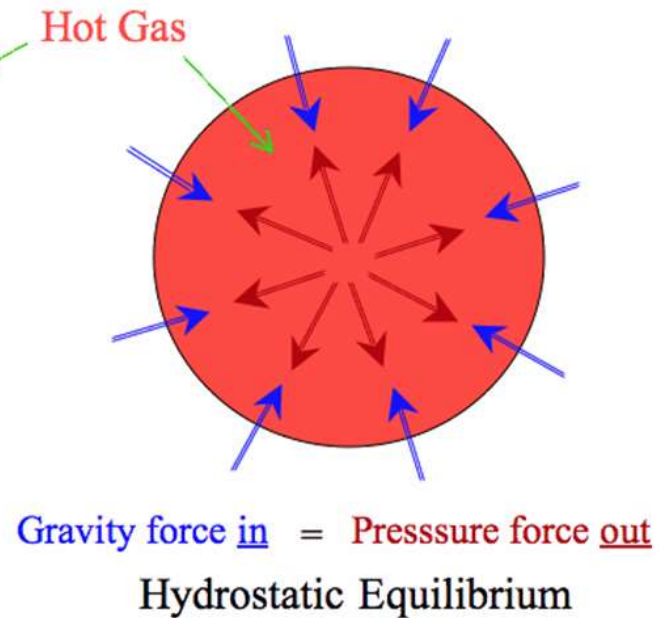
$L \sim 10^{43\text{-}46} \text{ erg/s} \sim 10^{-2} - 10^{-4} L_{\text{opt}}$

$M_{\text{gas}} \sim 5 \times M_{\text{gals}}$

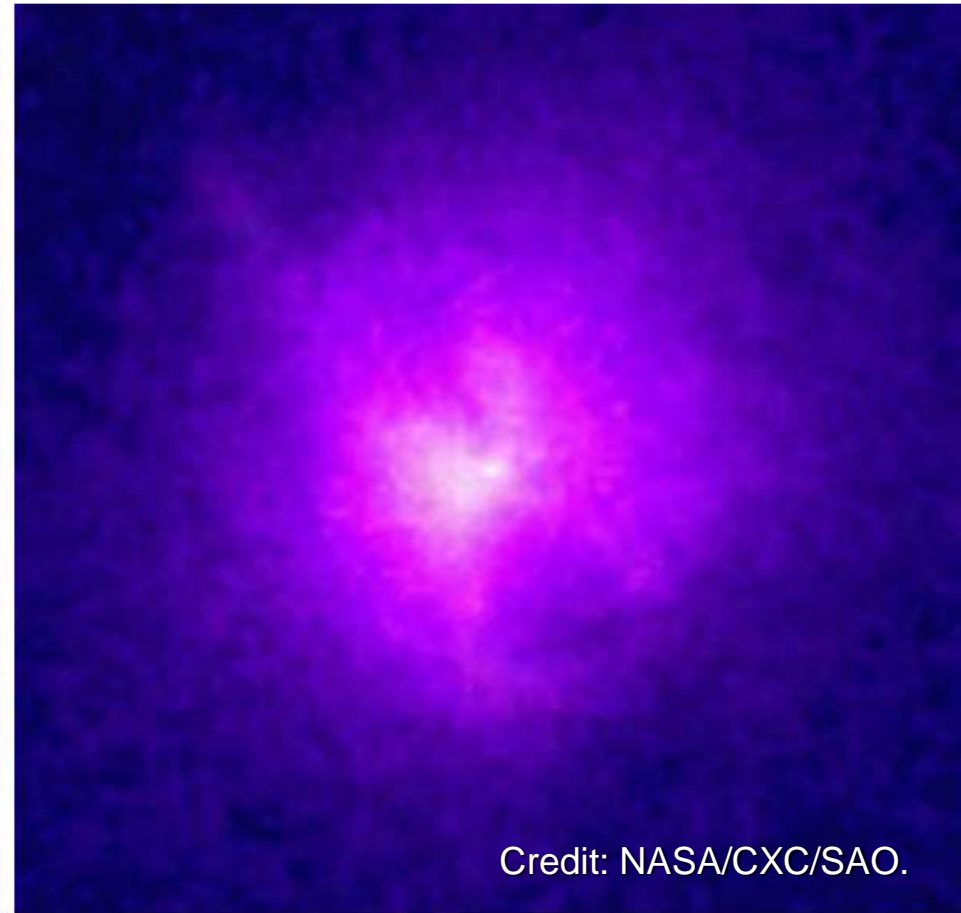
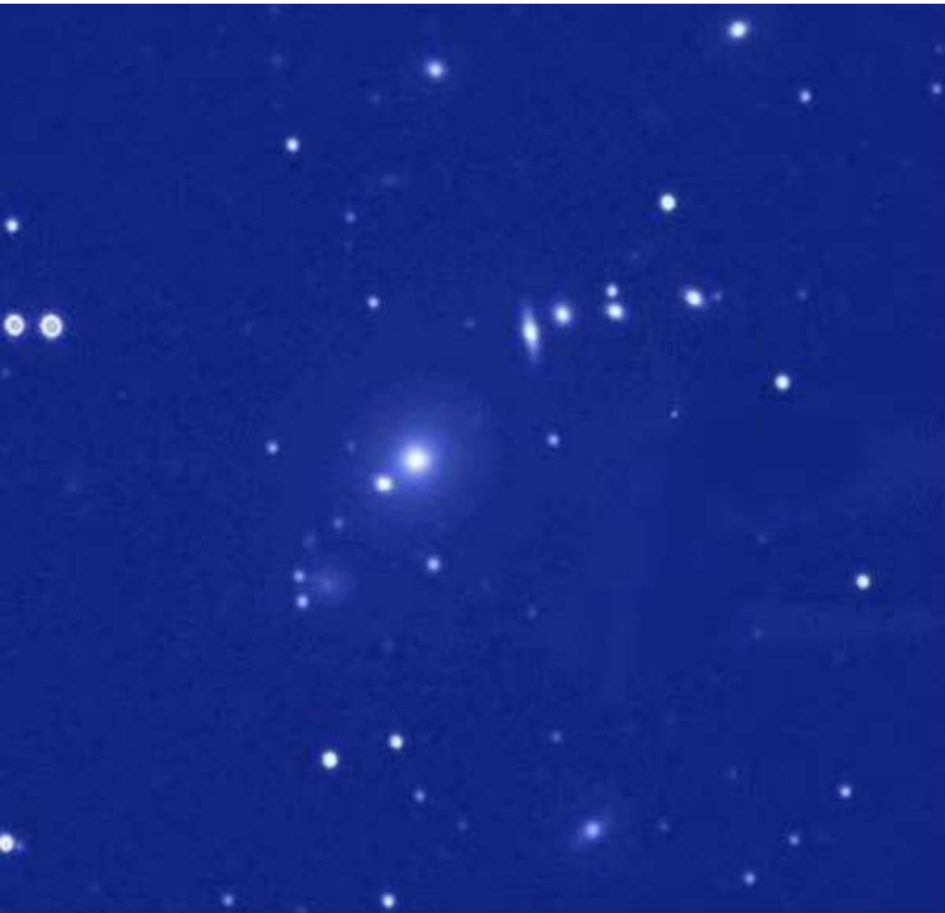
Gas metallicity $Z \sim 0.3 Z_{\odot}$ (enriched : not all primordial);



Coma cluster: X-ray (red), Optical (white)



Extended X-ray emission from clusters of galaxies was first observed in the early 1970's (G. M. Voit. astro-ph/0410173, 2004.)



Credit: NASA/CXC/SAO.

The Hydra A cluster of galaxies. Optical image from La Palma B.McNamara (left) and X-ray image from Chandra (right).

The physics of the principal constituents of clusters

● Dark Matter

Dominates in the total mass:

$$M_{\text{DM}} \sim 4 \times M_{\text{gas + gals}}$$

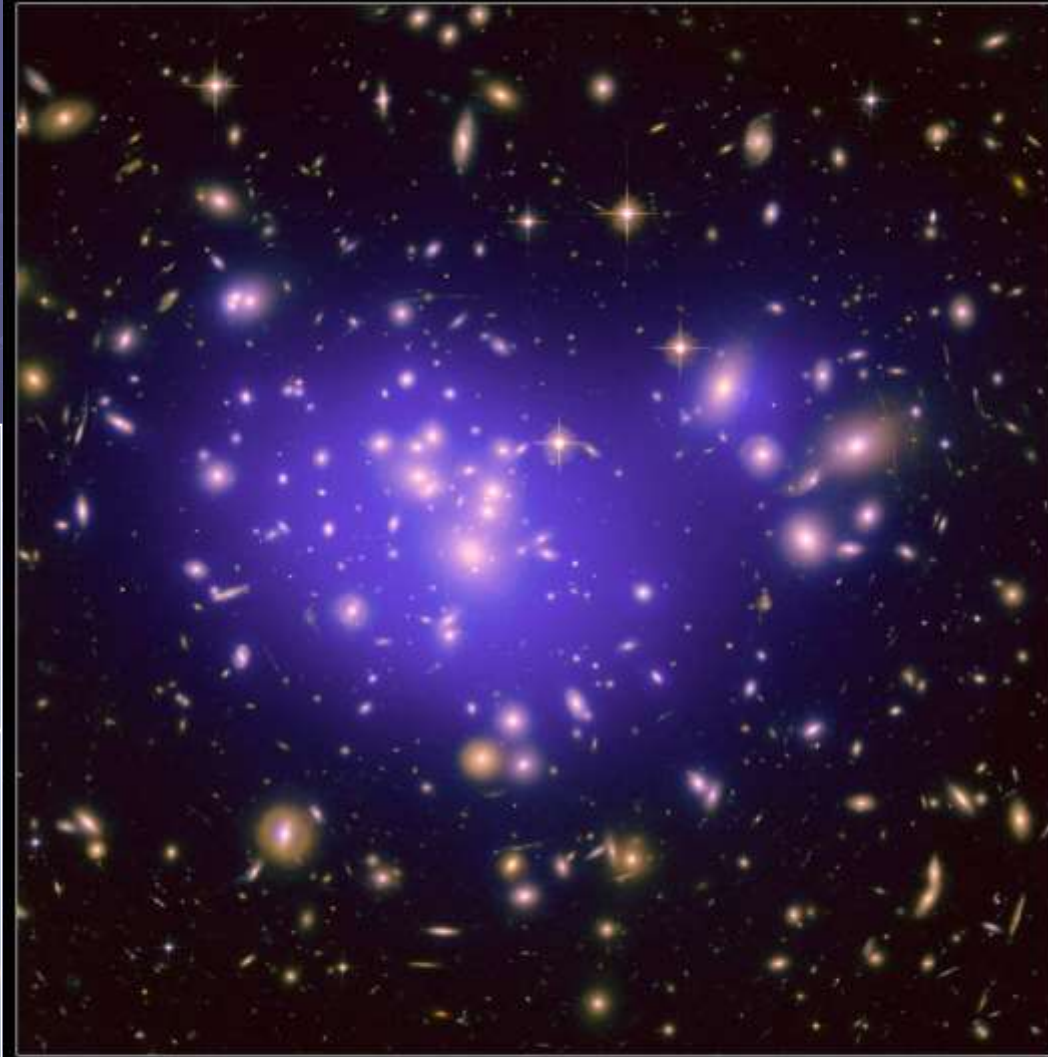
Taking into account

$$M_{\text{gas}} \sim 5 \times M_{\text{gals}}$$

$$M_{\text{DM}} \sim 24 \times M_{\text{gals}}$$

Dark Matter Map in Galaxy Cluster Abell 1689

HST ACS/WFC

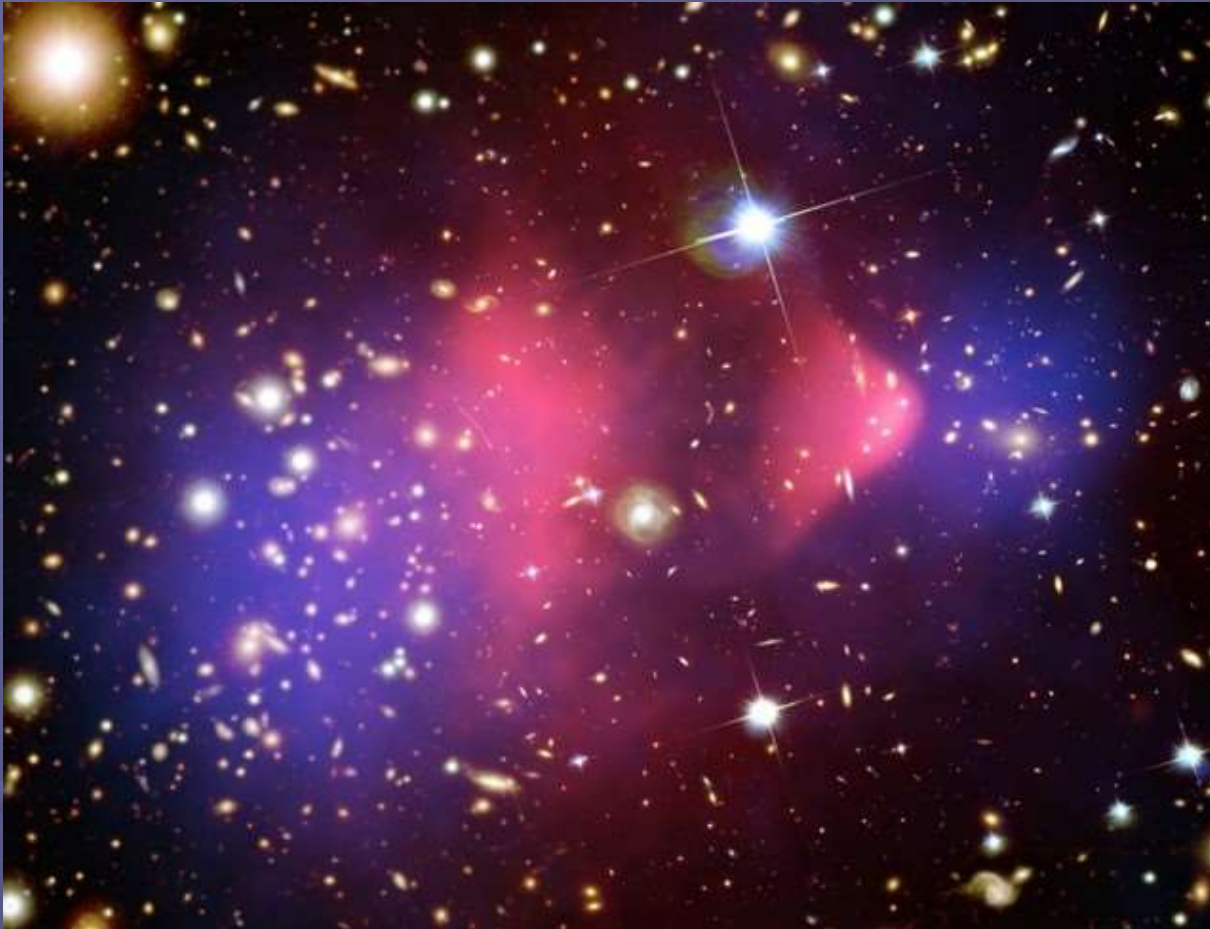


NASA, ESA, E. Jullo (Jet Propulsion Laboratory), P. Natarajan (Yale University),
and J.-P. Kneib (Laboratoire d'Astrophysique de Marseille, CNRS, France)

STScI-PRC10-26

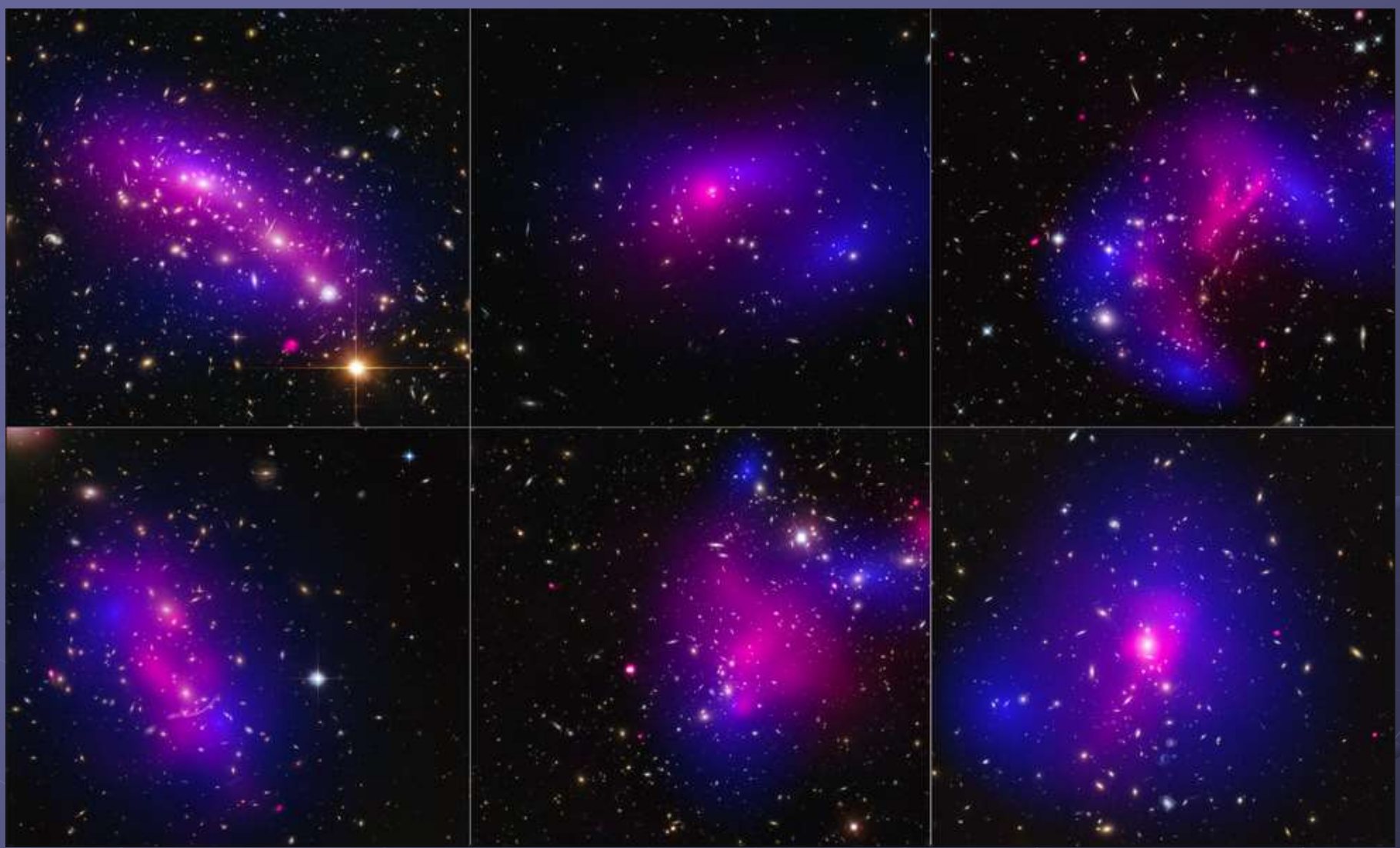
↔ CL0024+17. The gravity map is superimposed on a Hubble image of the cluster.

1E 0657-558 Bullet Cluster: composite image of X-ray (pink) and weak gravitational lensing (blue) of the famous Bullet Cluster of galaxies, $z = 0.3$



X-ray exposure time
was 140 hours

X-ray: NASA/CXC/CfA/ M.Markevitch et al.; Lensing Map: NASA/STScI; ESO WFI;
Magellan/U.Arizona/ D.Clowe et al. Optical: NASA/STScI;
Magellan/U.Arizona/D.Clowe et al.



The images of six different galaxy clusters taken with NASA's Hubble Space Telescope and Chandra X-ray Observatory (pink) show dark matter (blue) in collided galaxy clusters.

A total of 72 large cluster collisions were studied.

Credits: NASA and ESA

Morphology of Galaxy Clusters

Classification schemes of Galaxy Clusters based to one of several possible properties: viz shape, richness, lumpiness, Hubble mix, dominant galaxy types, etc.

Beginning approaches were:

1) “rich” clusters vs. “poor” clusters (Abell richness classes)

Poor clusters include galaxy groups and clusters with 100's of members. Rich clusters have 1000's of members. Higher density of galaxies.

2) “regular” clusters vs. “irregular” clusters (Abell R vs. I)

R-clusters have spherical shapes. Tend to be the rich clusters.

I - clusters have irregular shapes. Tend to be the poor clusters.

IR and RI are intermediate types

3) Compact, Medium-Compact, Open (Zwicky)

Comparison of Regular and Irregular Clusters – different facets

Property	Regular Clusters	Irregular Clusters
Richness	Rich	Poor
Concentration	High concentration of members toward cluster center	No marked concentration to a unique cluster center; often two or more nuclei of concentration are present
Symmetry	Marked spherical symmetry	Little or no symmetry
Collisions	Numerous collisions and close encounters	Collisions and close encounters are relatively rare
Types of galaxies	Brightest galaxies are elliptical and/or S0 galaxies. Cluster often centered about one or two giant elliptical galaxies	All types of galaxies are usually present Late-type spirals and/or irregular galaxies present
Diameter (Mpc)	Order of 1 - 10	Order of 1 - 10
Subclustering	No	Often present.
V_r dispersion	Order of 10^3 km/sec	Order of 10^2 - 10^3 km/sec
Mass (from Virial Theorem)	Order of $10^{15} M_{\odot}$	Order of 10^{12} - $10^{14} M_{\odot}$
Examples	Coma cluster (A1656); Corona Borealis cluster (A2065)	Virgo cluster, Hercules cluster (A2151)

More: Bahcall N.
arXiv:astro-ph/9611148.

Main classification schemes:

The **Bautz-Morgan (BM)** classification is based on brightness contrast between first- and second-ranked galaxies (*ApJ* **162**, L149, 1970)

- BM I single central dominant cD galaxy (A 2199)
- BM II several bright galaxies between cD and gE (Coma)
- BM III no dominant galaxy (eg Hercules)

Intermediate types are I-II and II-III

Some later **Oemler** (1974) recognised three types of cluster according to Hubble mix: "spiral rich" (eg Hercules); "spiral poor" (eg Virgo); "cD" (eg Coma);

López-Cruz at al. introduced the definition of a cD cluster, the complement to this class is called a non-cD cluster.

(*ApJ* **194**, 1, 1974. *ApJ*, **475**, L97, 1997)

The Rood and Sastry (RS) classification is based on the projected distribution of the brightest 10 members.

cD - single dominant cD (elliptical) galaxy (A2029, A2199)

B - dominant binary, (Coma)

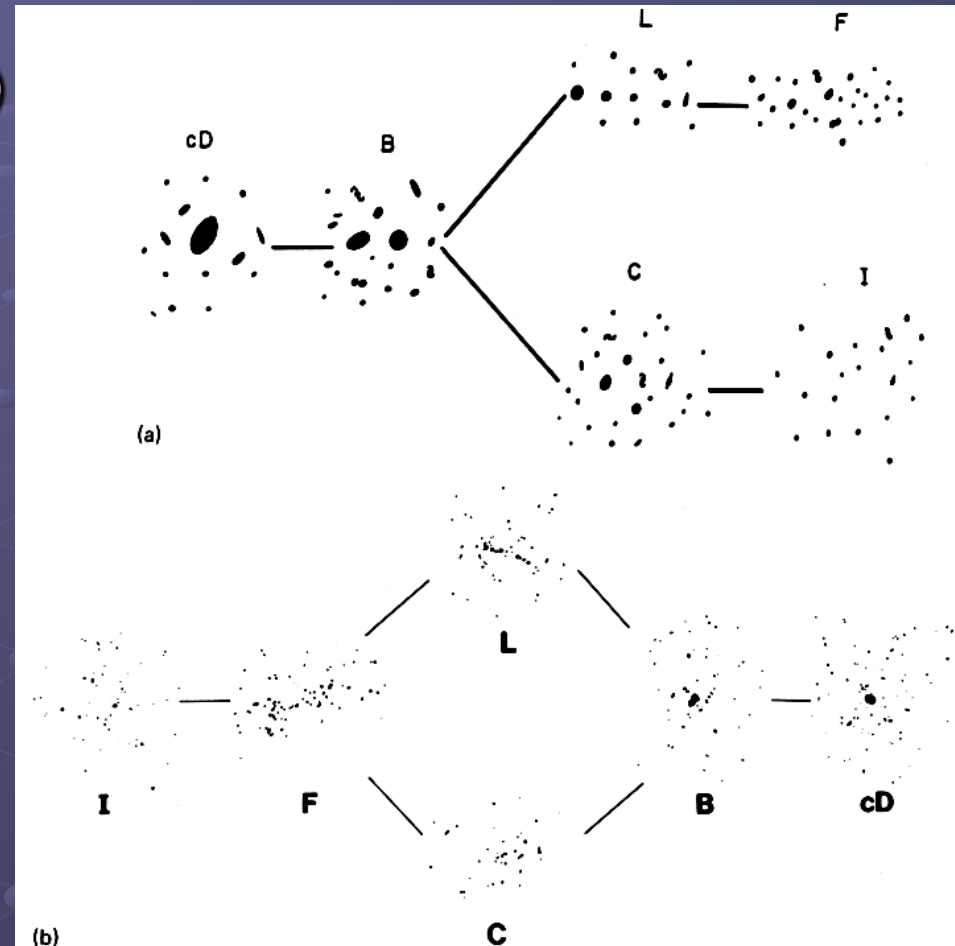
L - linear array of galaxies (Perseus)

C - single core of galaxies

F - flattened (IRAS 09104+4109)

I - irregular distribution (Hercules)

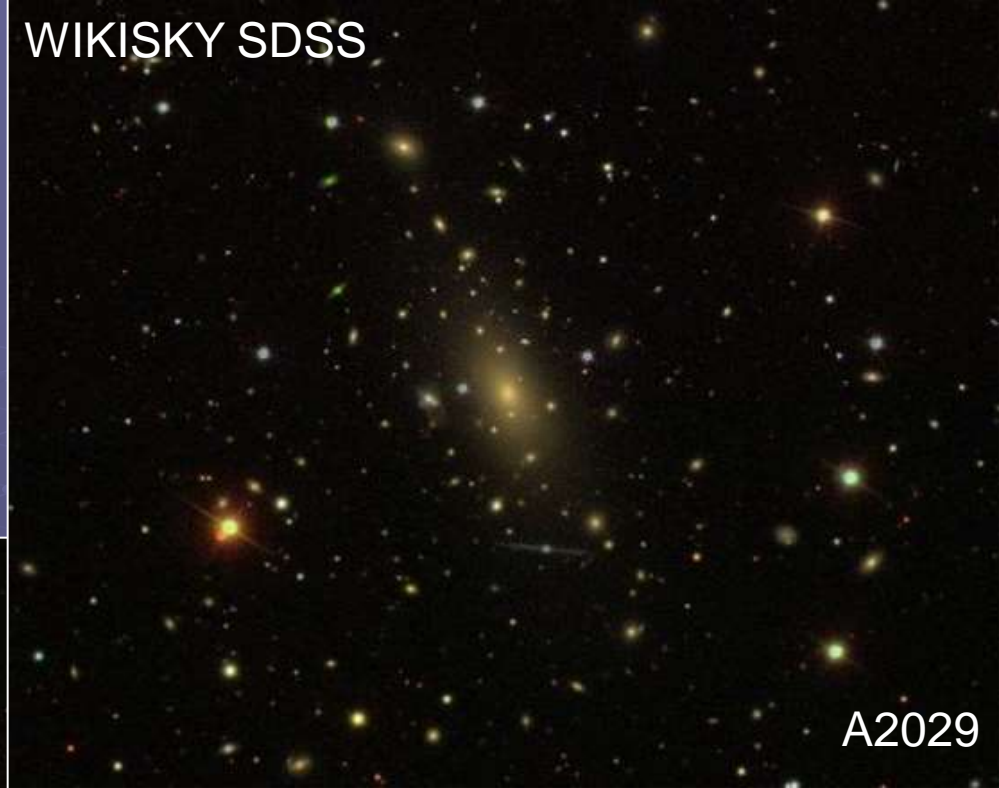
(*PASP* 83, 313, 1971, *AJ* 87, 7, 1982).



RS 1971 "tuning-fork" (a) and revised R-S (b) cluster classification scheme (1982).

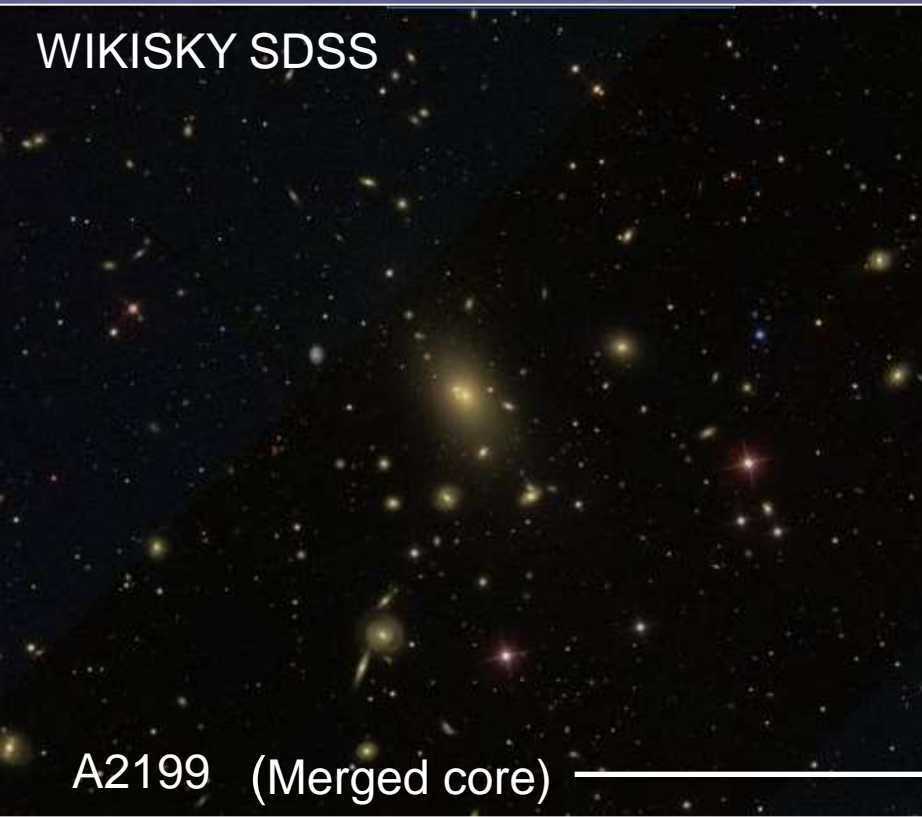
BM I, RS cD, R...

WIKISKY SDSS



A2029

WIKISKY SDSS



A2199 (Merged core)



BM II, RS B...

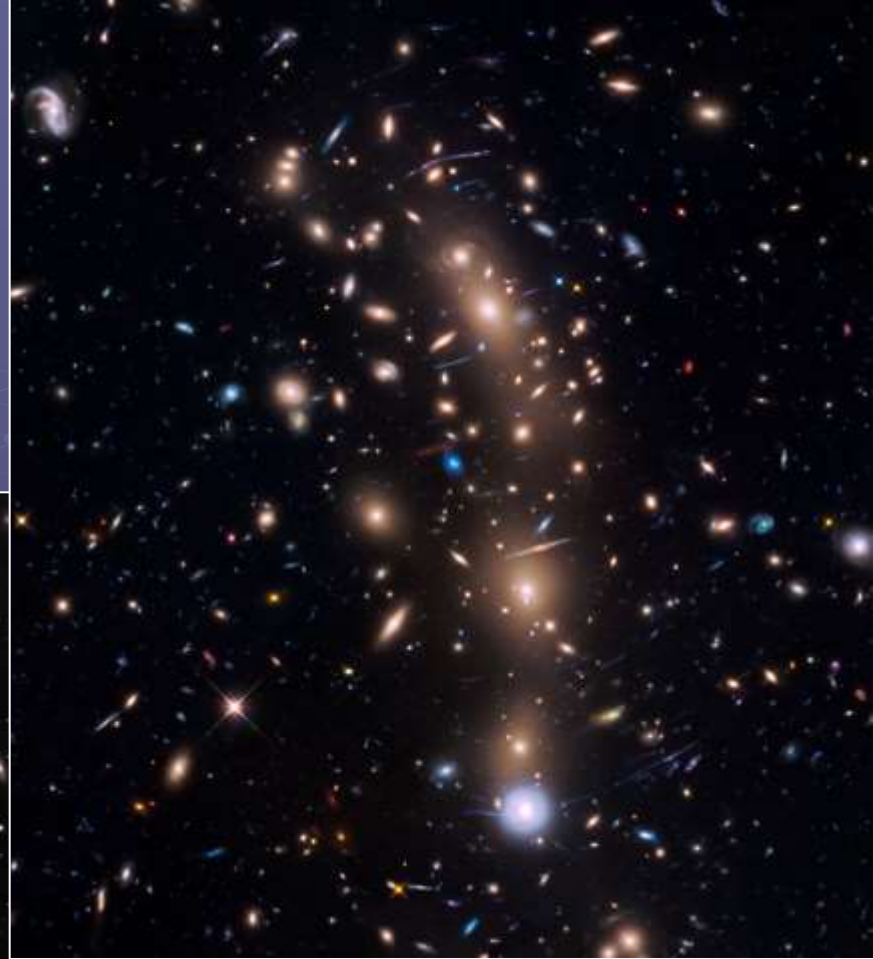
Coma

Image courtesy of Adam Block.



BM II, RS L...

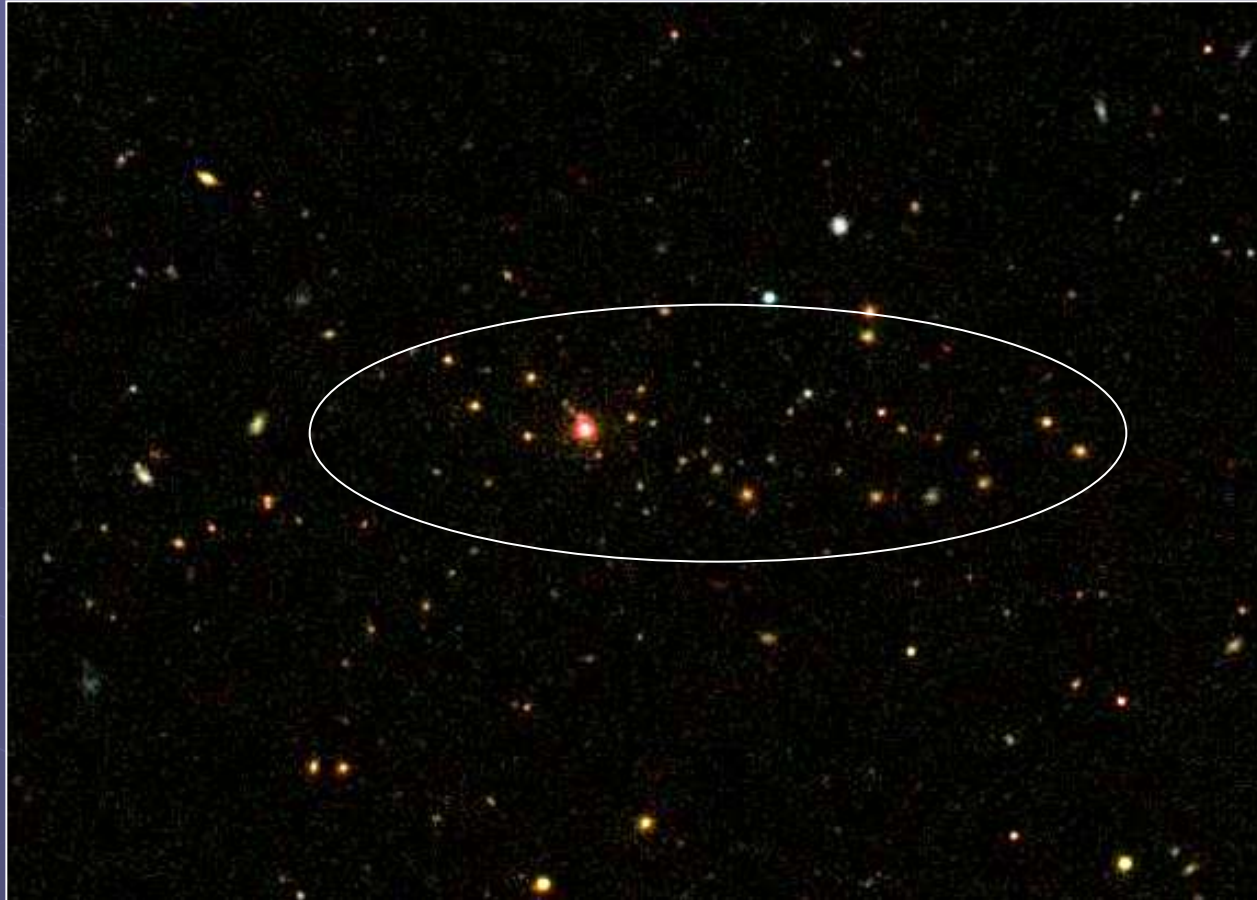
WIKISKY SDSS



Galaxy cluster MACS
J0416.1-2403, courtesy
Hubble Frontier Fields

The Perseus Galaxy Cluster (Abell 426)

BM III, RS F



IRAS 09104+4109

WIKISKY SDSS

BM III, RS I



WIKISKY SDSS

Hercules

Comparison of the RS and BM types

The RS and BM schemes are in agreement and complement each other. It seems there is a primary factor which defines a cluster : its degree of relaxation. From least relaxed to most relaxed we have :

BM : III \Rightarrow II \Rightarrow I

RS : I \Rightarrow F \Rightarrow C (L) \Rightarrow B \Rightarrow cD

A number of other properties follow this sequence :

Hubble type mix :	Spiral rich	Spiral Poor	Elliptical rich
Overall Shape :	Irregular	Intermediate	Spherical
X-ray Luminosity :	low	Intermediate	High

One can suppose that this sequence reflects, at least in part, stages in cluster evolution :

least evolved \Rightarrow intermediate \Rightarrow most evolved

L and F clusters can note to anisotropy.

For study the PF Galaxy clusters (MRSS) one more scheme was proposed. Adapted morphological classes based on 3 parameters: concentration, the single of preference plane (flatness) and BG positions:

- concentration **C** – compact, **I** – intermediate and **O** – open;
- flatness **L** – line, **F** – flat and no sign of flatness (no symbol);
- using Bright Cluster Members role **cD** and **BG**;
- other peculiarities are noted as **P**.

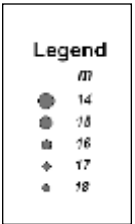
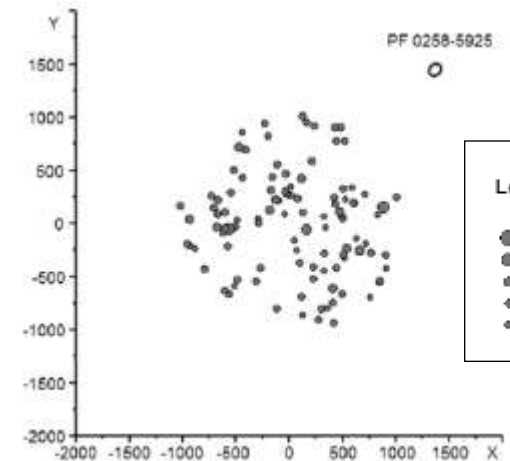
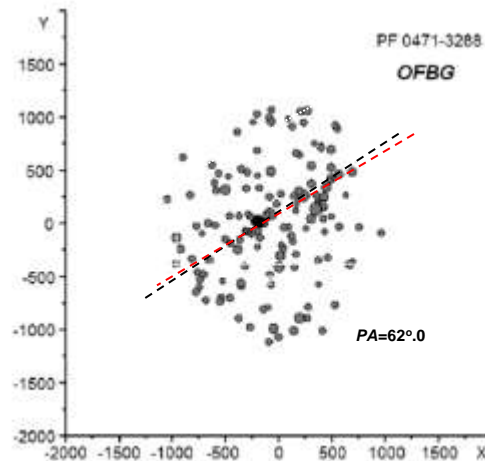
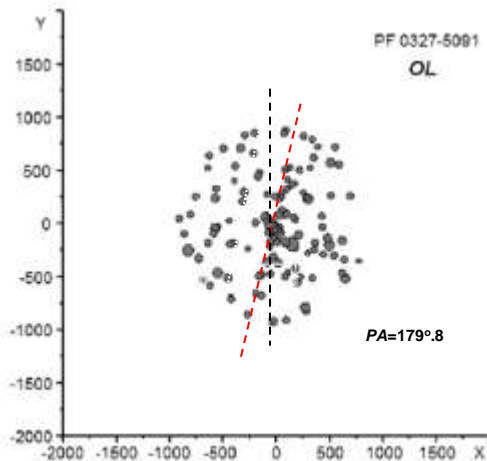
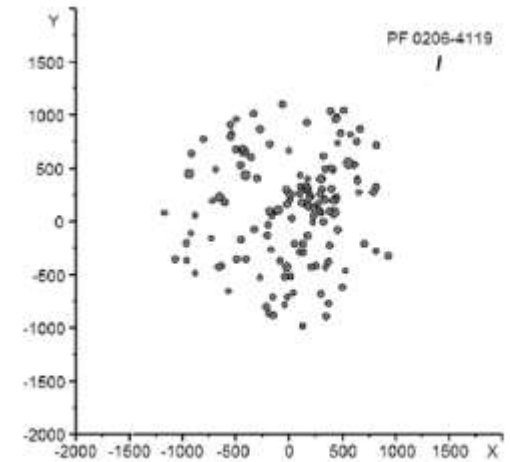
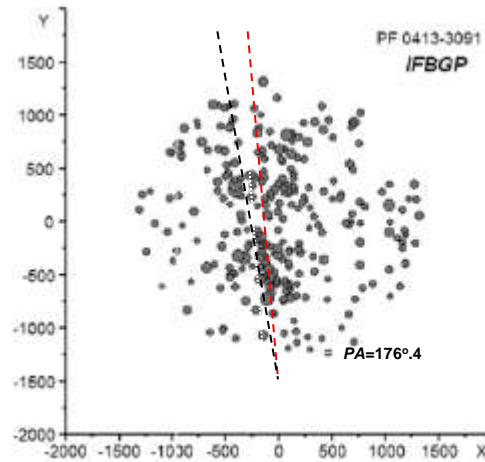
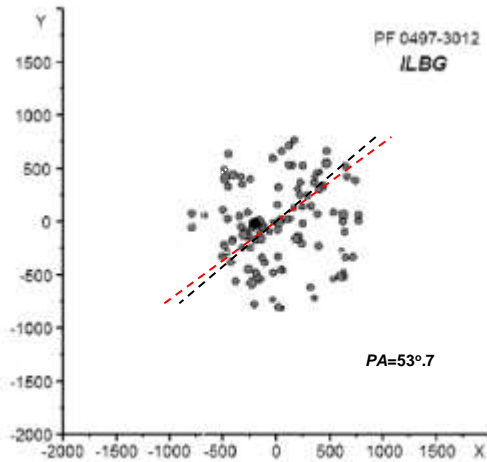
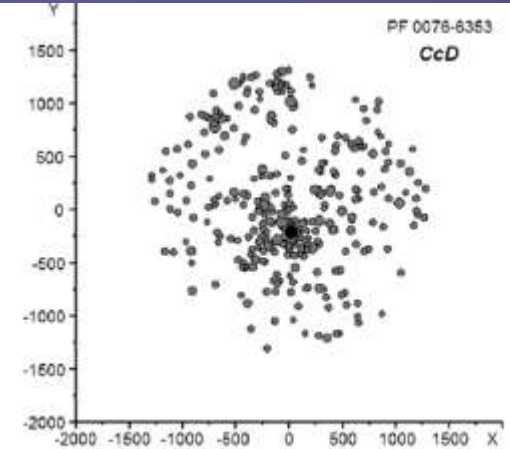
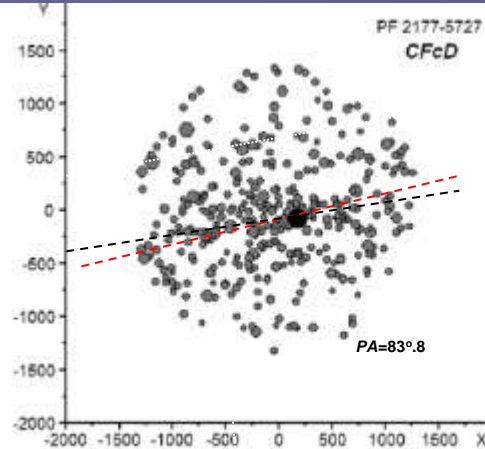
The parameters can be combined.

Property \ Class	Regular	Intermediate	Irregular
Zwicky type	Compact	Medium-Compact	Open
Bautz-Morgan type	I, I-II, II	(II), II-III	(II-III), III
Rood- Sastry type	cD, B, (L,C)	(L), (F), (C)	(F), I
López-Cruz	cD	non-cD	non-cD
Symmetry	Spherical	Intermediate	No
Central concentration	High	Moderate	Very little
Central profile	Steep	Intermediate	Flat
Adapted types (Panko, 2013)	C, (CF), CcD, CBG	I, IBG, IL, IF, IP	O, OBG, OL, OF, OP,

Types of clusters

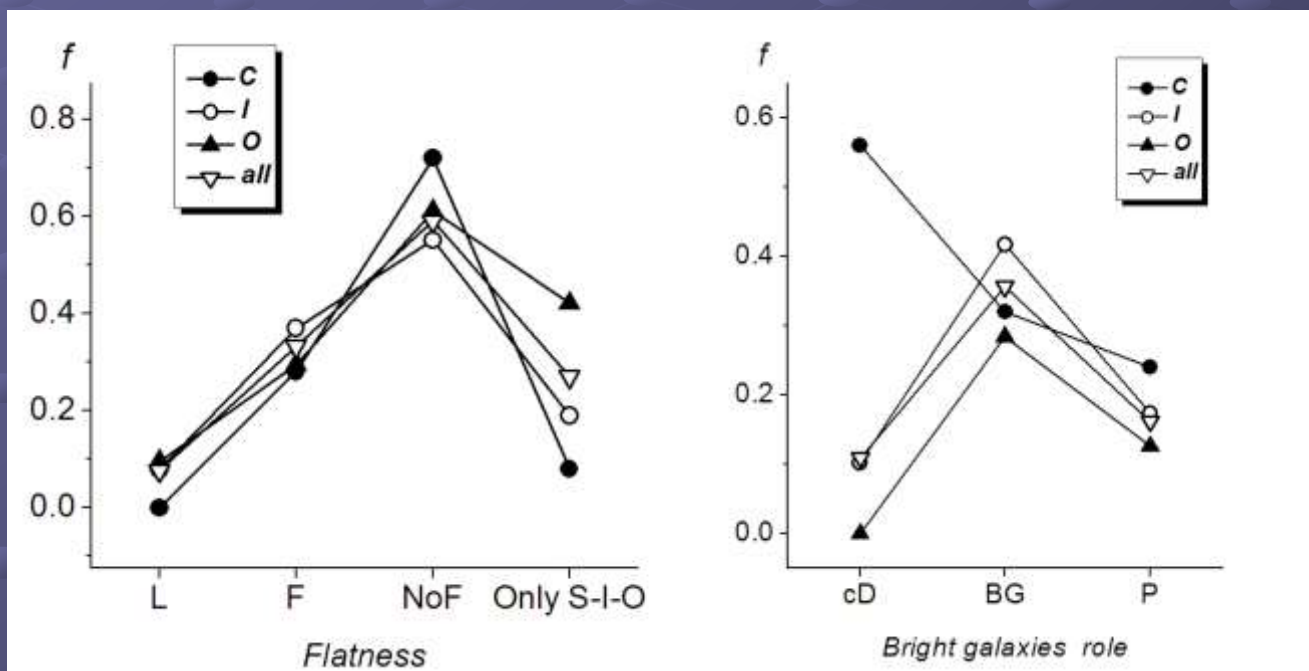
Note a correlation between position angle for the major axes of the best-fit ellipse (black) and the direction of the preferred plane (red) in L and F clusters.

CL type was not found.



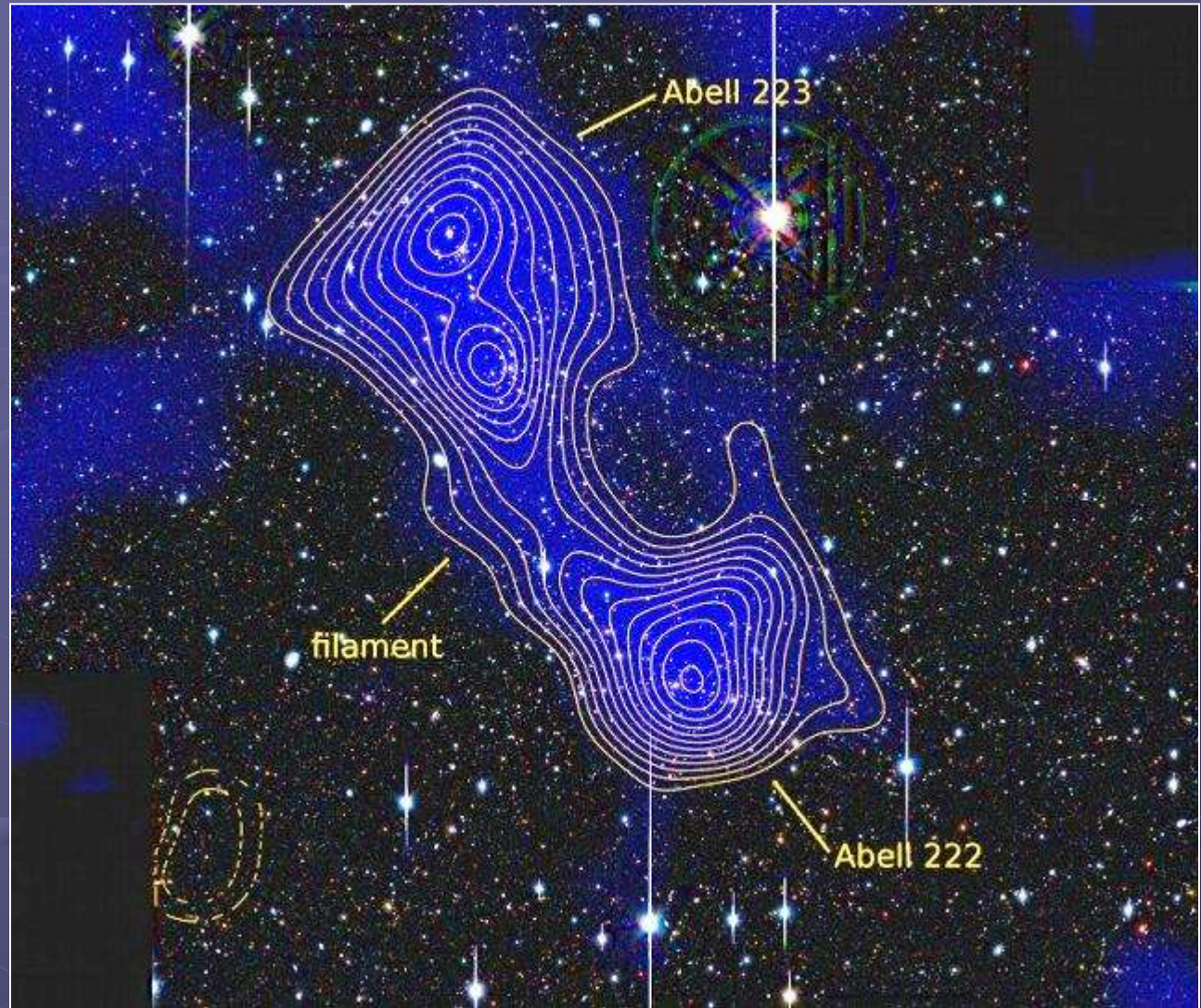
From the distributions of the frequencies of clusters with different morphology one can see that concentration and flatness are independent morphological criteria. The frequencies of L and F types are similar in C-I-O subsets.

In contrast, the role of BCMs is strongly connected with cluster concentration: the number of cD clusters is greatest in C-type.



Clusters are prolate or triaxial; richer clusters are less elongated, so C-I-O consecution with L-F marks divides clusters by shape and concentration.

The anisotropy in L or F clusters can be connected with dark matter filaments.

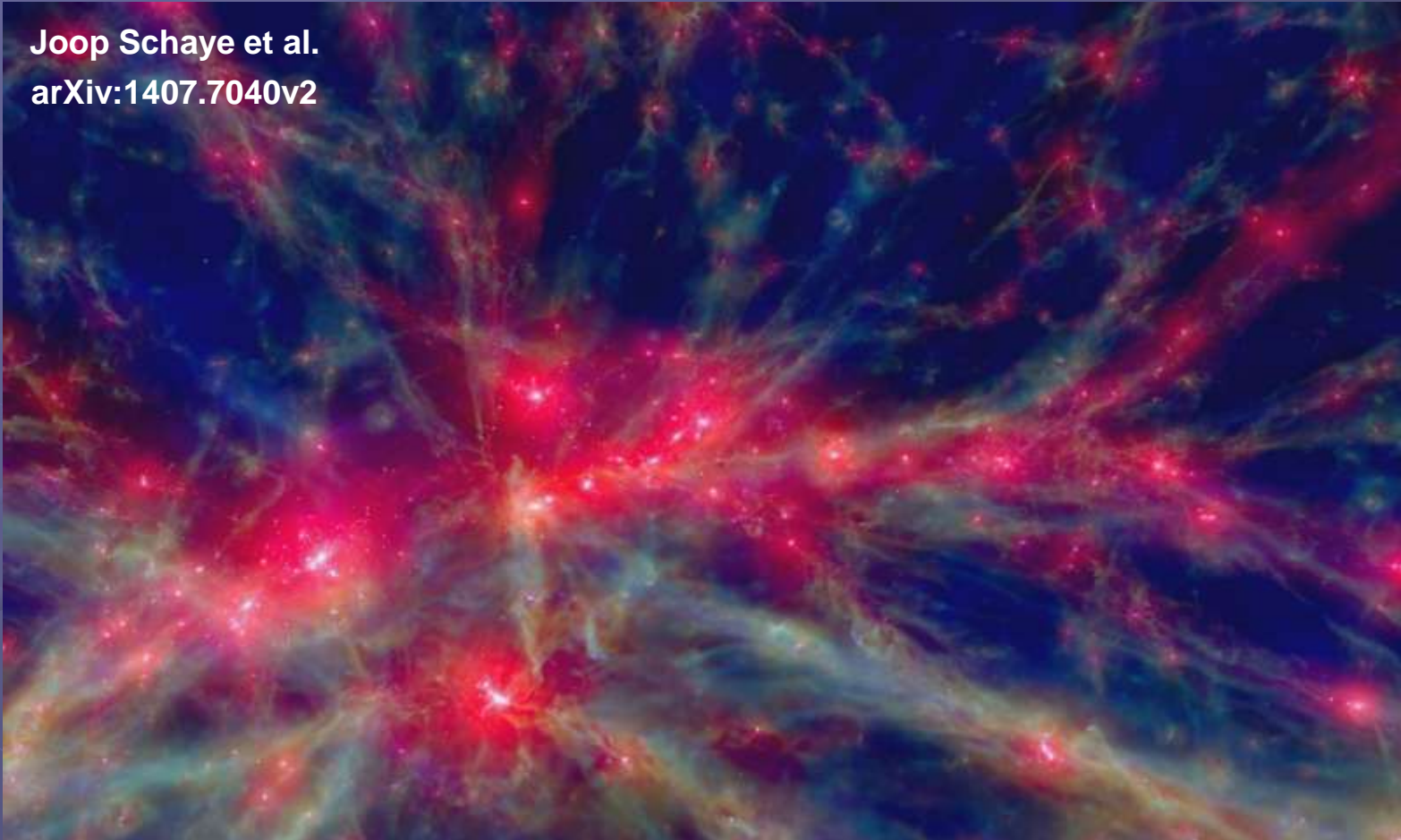


Jörg Dietrich et al. found the dark matter filaments (blue) in A222 and A223 clusters.

<http://arxiv.org/abs/1207.0809>

EAGLE (Evolution and Assembly of GaLaxies and their Environments)

Joop Schaye et al.
arXiv:1407.7040v2



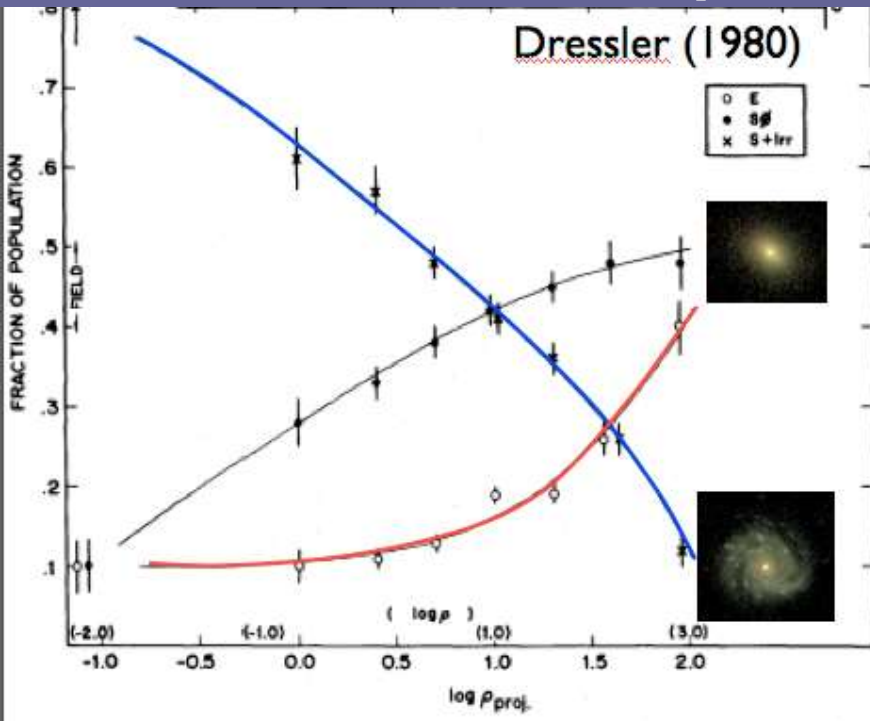
A 100x100x20 cMpc slice through the Ref-L100N1504 simulation at $z=0$. The intensity shows the gas density while the color encodes the gas temperature using different color channels for gas with $T < 10^{4.5} \text{K}$ (blue), $10^{4.5} \text{K} < T < 10^{5.5} \text{K}$ (green), and $T > 10^{5.5} \text{K}$ (red).

Hubble mix – was analyzed for nearest clusters

At first Shapley in 1926 noted to the different galaxy content of the Virgo and the Coma cluster. Ten years after, Hubble first hinted at the existence of a morphology-density relation. Then was found:

Property/Class	Regular	Intermediate	Irregular
Zwicky type	Compact	Medium-Compact	Open
Bautz-Morgan type	I, I-II, II	(II), II-III	(II-III), III
Rood-Sastry type	cD,B, (L,C)	(L),(F),(C)	(F), I
Central concentration	High	Moderate	Very little
Content	Elliptical-rich	Spiral-poor	Spiral-rich
E:S0:S ratio	3:4:2	1:4:2	1:2:3
Examples	A2199 (z=0.030), Coma (A1656) (z=0.023)	A194 (z=0.018), A539 (z=0.028)	Virgo, A1228 (z=0.035)

The Morphology – Density Relation



The higher the density of galaxies, the higher the fraction of elliptical – for 55 clusters and 15 fields (*ApJ*, **236**, 351, 1980).



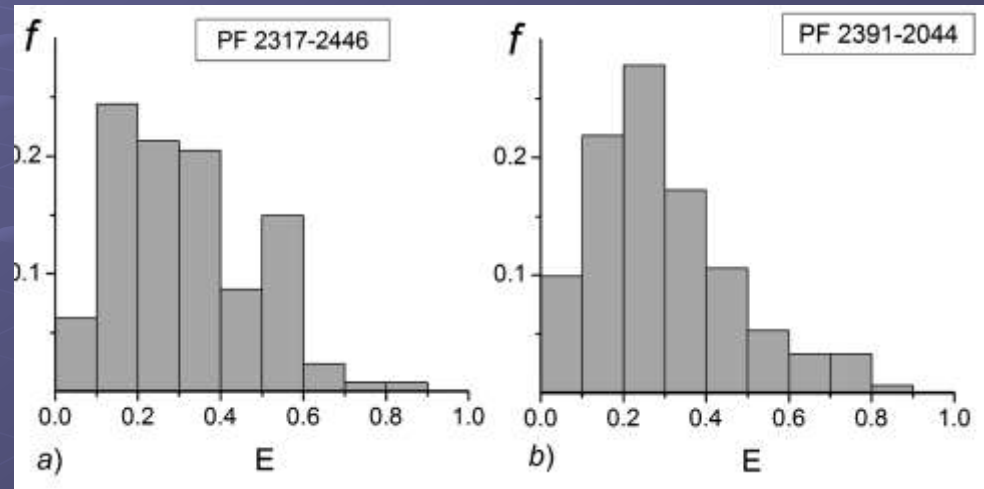
Virgo cluster: spiral galaxies in the central part



Coma cluster: thousands of galaxies, high elliptical fraction

For big data sets (~1200000 MRSS galaxies) we have no Hubble types. However, for these galaxies was calculated the ellipticity – in the projection to the astroplate. One can assume the ellipticity as parameter for rough estimation of morphology.

MRSS galaxies in clusters with different morphological types show two kinds of ellipticity distributions: bimodal (a) for E-poor and single-mode (b) for E-rich clusters.



So, both global cluster conditions and local galaxy density play roles. Fasano et al. (2000) found the trends in S0:E and S0:S indicated a morphological evolution; as redshift decreases, the S0 (lenticular) population tends to grow at the expense of regular spiral galaxies.

Can we say about evolution of morphology-density relation?

Only with HST has it been possible to study morphology of galaxies at high- z ($z \sim 0.5$; lookback times $\sim 6-8$ Gyr).

This gives insight into whether the morphology-density relation stems from galaxy formation or galaxy evolution.

HST studies find :

$f(E)$ is the same as low- z ;

$f(S0)$ is lower by factor 2-3;

$f(Sp)$ is higher by factor 2-3.

The morphology-density relation is absent in irregular clusters.

We conclude from this:

Ellipticals formed earlier (at even higher z).

For Ellipticals, the density at formation is most important.

Spirals are converted into S0s, in an ongoing process which depends on density (still to be identified).

These results are broadly consistent with the "Butcher-Oemler Effect" (1978) in which the fraction of blue galaxies is found to be higher in distant clusters.

This is an active area of research, with many details and uncertainties.



So, can we say about evolution of morphology-density relation?

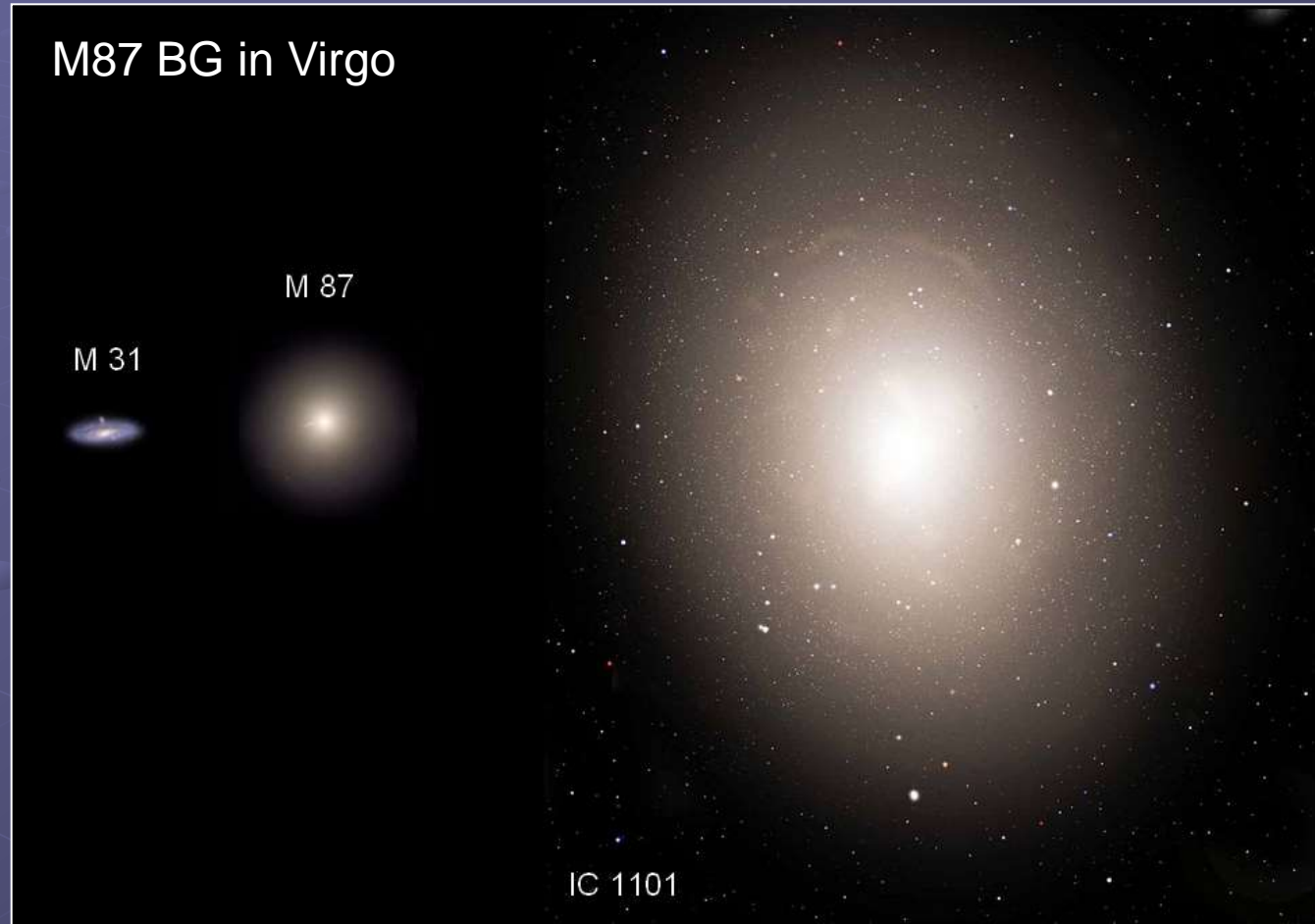
YES!

Credit:
 NASA, ESA, Sloan Digital Sky Survey, R. Delgado-Serrano and F. Hammer (Observatoire de Paris)



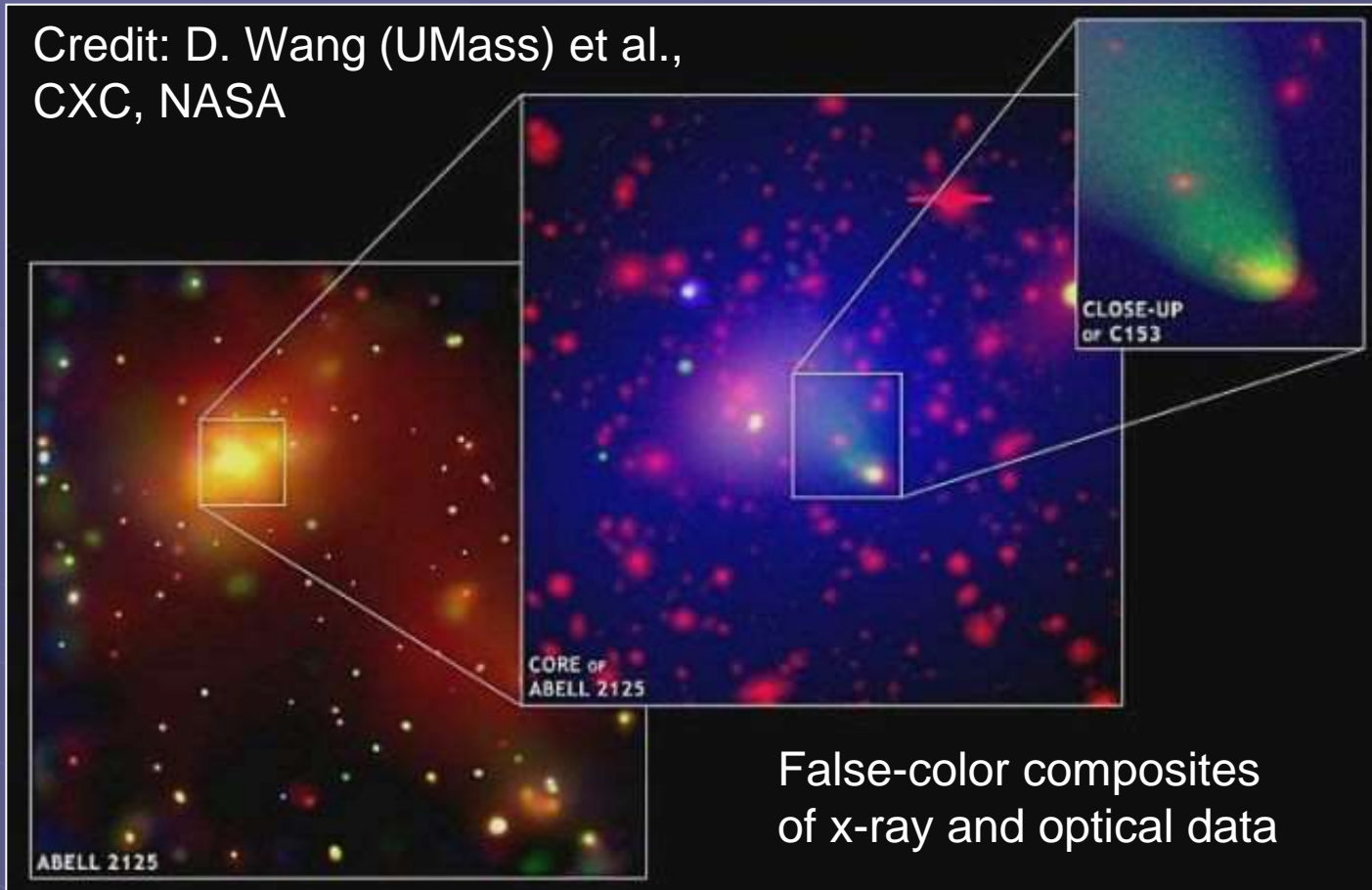
cD galaxies are anomalies in the galaxy population. They are:

- very luminous Elliptical galaxies ($L_{cD} \approx 10 \times L_G$), i.e. unusually bright;
- very large with an extended halo (50 - 100 h^{-1} kpc);
- there is alignment of cD galaxy and parent cluster;
- located at the spatial and velocity center of the cluster.;
- Images often show double/triple merging nuclei within cDs.



File usage on Commons
Fernando de Gorocica

Credit: D. Wang (UMass) et al.,
CXC, NASA



cD galaxies have a qualitative different formation history than other cluster galaxies. Their origin can be connected with mergers of cluster galaxies in the cluster core. A comet-like tail of glowing gas from galaxy C153, 200'000 light-years long, on the core of galaxy cluster Abell 2125 is the stage of "galactic cannibalism". The series of images illustrate a possible history of cD galaxies grow.

Credits: X-ray: NASA/CXC/Univ of Missouri/M.Brodwin et al;
Optical: NASA/STScI; Infrared: JPL/CalTech Jan. 7, 2016

IDCS J1426.5+3508, z=1.75

It is the highest redshift
strong lensing cluster known
and the most distant cluster
for which a weak lensing
analysis has been
undertaken

$$M = 2.3^{+2.1}_{-1.4} \times 10^{14} M_{\odot}$$

Wenli Mo et al., arXiv:1601.07967

This image of IDCS 1426 J1426.5+3508 combines data taken by three major NASA telescopes. The off-center core of X-rays is shown in blue-white near the middle of the cluster, and was captured by Chandra. Visible light from the Hubble Space Telescope, and infrared light from Spitzer is shown in red.

CL J1449+0856, $z = 2$



Composite image, about 100 arc minutes on a side, shows the X-ray emission (in purple) coming from the diffuse intra-cluster medium of the galaxy cluster CL J1449+0856 as detected by XMM-Newton.

The redshift was found to be 2.00. The cluster luminosity is approximately 7×10^{43} erg/s in the soft X-ray energy range (0.1-2.4 keV). An estimated mass of $5-8 \times 10^{13}$ solar masses.

Copyright: ESA/ESO/Subaru/R. Gobat et al.

R. Gobat et al., [A&A 526, A133, 2011](#)
[arXiv:1305.3576, 2013](#)

The all aspects of study of galaxy clusters are useful
for our knowledge of Universe and so Interesting.

THANK YOU!

2dF

LEVEL 5

<http://ned.ipac.caltech.edu/level5/>

A Knowledgebase for Extragalactic Astronomy and Cosmology

This lecture was prepared use of the NASA/IPAC Extragalactic Database (NED) which is operated by the Jet Propulsion Laboratory, California Institute of Technology, under contract with the National Aeronautics and Space Administration.



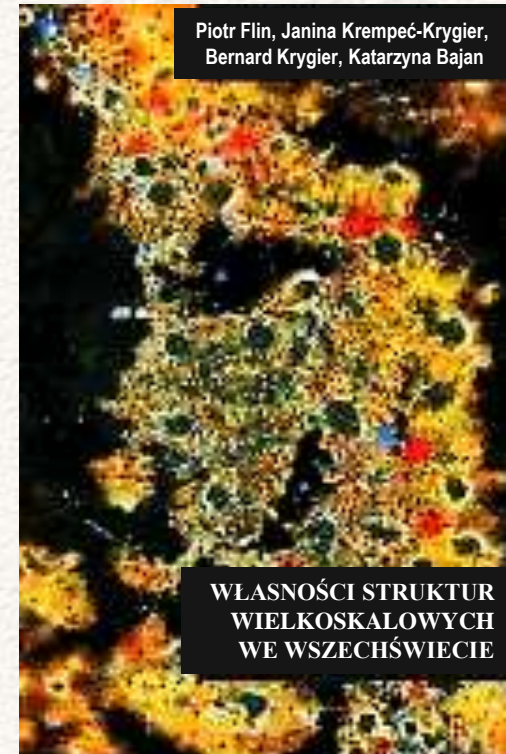
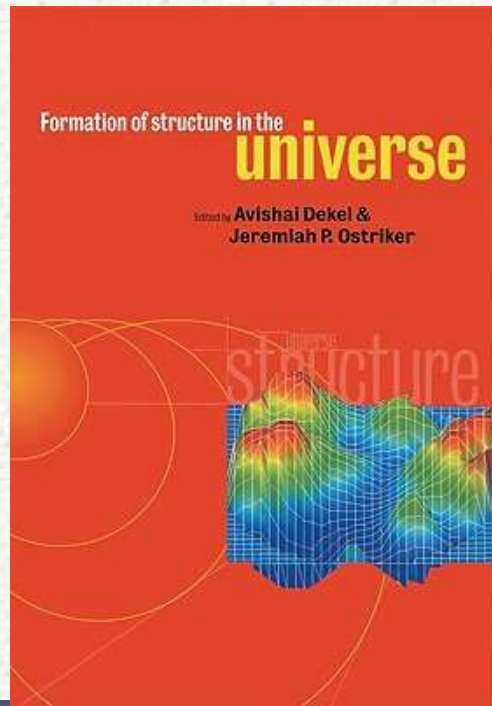
Principal Investigator
Dr. Barry F. Madore

Caltech and Carnegie
Pasadena, California, USA

Under the sponsorship of NASA's
Applied Information Systems Research Program (AISRP)

NASA/IPAC Extragalactic Database

Professor
Mark Whittle, Ph.D.
University of Virginia
– some fragments of
"EXTRAGALACTIC
ASTRONOMY" were used



Piotr Flin, Janina Kremeć-Krygier,
Bernard Krygier, Katarzyna Bajan

WŁASNOŚCI STRUKTUR
WIELKOSKALOWYCH
WE WSZECHŚWIECIE